ALMA MATER STUDIORUM – UNIVERSITÀ DI BOLOGNA

SCUOLA DI INGEGNERIA E ARCHITETTURA

CORSO DI LAUREA MAGISTRALE IN CIVIL ENGINEERING

DIPARTIMENTO DI INGEGNERIA CIVILE,AMBIENTALE E DEI MATERIALI

TESI DI LAUREA

in

Advanced Hydrosystems Engineering

TOXICITY ASSESSMENT OF INDUSTRIAL- AND SUNSCREEN-DERIVED ZnO NANOPARTICLES

CANDIDATO
Spisni Eleonora

RELATORE:
Chiar.mo Prof. Andrea Bolognesi

CORRELATORE:
Prof. Sung Hee Joo

Anno Accademico 2015/2016

Sessione I

Keywords
Nanoparticles
Sunscreen
Toxicity
Diatom

TABLE OF CONTENTS

Abstract

Lo scopo della presente tesi è l'analisi della tossicità di nanoparticelle di ossido di zinco (nano-ZnO) verso gli organismi acquatici. In particolare, il presente studio valuta per la prima volta l'inibizione della crescita della diatomea Thalassiosira pseudonana indotta sia da nanoparticelle di dervazione industriale, che da nanoparticelle auto-estratte in laboratorio da un filtro solare. Gli esperimenti, condotti presso il Laboratorio di Ingegneria dell'Università di Miami, hanno mostrato che la tossicità indotta dalle nanoparticelle di ossido di zinco è influenzata dal tipo di nanoparticelle, nonché dalla loro concentrazione nella soluzione acquosa e dal tempo di esposizione. In particolare le nanoparticelle di derivazione industriale, più piccole rispetto alle nanoparticelle estratte dal filtro solare, hanno indotto un'inibizione della crescita superiore, specialmente a concentrazioni inferiori. Questo andamento suggerisce che ad alte concentrazioni la tossicità di nano-ZnO potrebbe essere influenzata dall'aggregazione di nanoparticelle (indipendentemente dalle dimensioni di partenza delle nanoparticelle), mentre a concentrazioni inferiori la tossicità potrebbe essere influenzata dalle dimensioni di partenza delle nanoparticelle, così come dal tipo di nanoparticelle e dal tempo di esposizione.

Chapter 1 - Introduction

Nanotechnology is the manipulation of matter with at least one dimension, sized from 1 to 100 nanometers[1]. At the nanoscale, the properties of particles may change in unpredictable ways and, thanks to this peculiar property, the field of nanotechnology is nowadays very broad, as it includes molecular biology and organic chemistry [2,3], materials science and engineering [4–7] and cosmetics [8–10]. As can be guessed, nanoparticles can contribute to stronger, lighter and "smarter" surfaces and systems.

At the macroscale, zinc oxide [11,12] is an inorganic compound, a white powder insoluble in water but soluble in acid or alkaline solutions (Fig.1.1a). In nature it can be found in its mineral form called zincite (Fig.1.1b), but the majority of zinc oxide is produced synthetically; crystalline zinc oxide shows piezoelectricity properties and is thermochromc: It changes color from white to yellow when heated and back. It has good transparency and refractive index, therefore it is often used as white pigment in many commercially available products.

a) b)

Figure 1.1. a) Powder of zinc oxide ZnO [13], b) Zincite[14].

The study "Industrial production quantities and uses of ten engineered nanomaterials in Europe and the world" by Piccinno et al. (2013)[15], assesses, by means of a survey among experts, worldwide and European production and use of nano-ZnO. In Figure 1.2 it is possible to see the results of the survey. In particular, nano zinc oxide (nano-ZnO) is estimated to have a worldwide production of 550

tons per year (with a 25th and 75th percentile of 55 tons per year) and a European production of 55 tons per year (with a 25th and 75th percentile of 5.5 and 28000 tons per year, respectively). The product distribution is estimated to be 70% in cosmetics (including sunscreens) and 30% in paints.

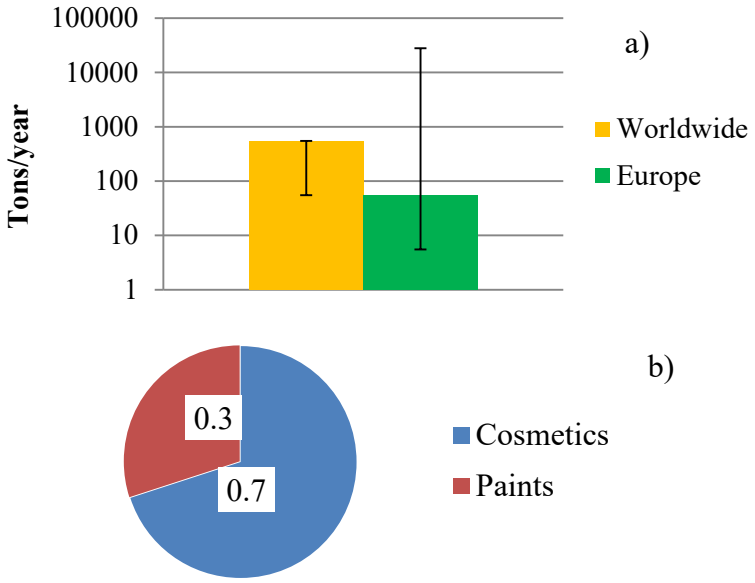

Figure 1.2. a) Estimated production of nano-ZnO and b) its distribution among consumer products[15].

Nano-ZnO has the potential to improve these products, however, it must also be considered that nanotechnologies raise concerns about their toxicity and environmental impact. According to Bystrzejewska-Piotrowska et al. (2009)[16] and Gebel et al. (2014)[17], three different causes (non-mutually exclusive) of toxicity from nanomaterials can be identified as follows:

- First, the toxicity can be due to the chemical element or compound itself (e.g., heavy metals);

- Second, the toxicity can be due to the small size of the particles, that both guarantees a large surface area per unit volume and fosters the nanoparticle sticking to other cells; and

- Third, the toxicity can be due to the shape of the particles (e.g., carbon nanotubes CNT can pierce membranes).

Regarding health, nanoparticles may enter the human body primarily through inhalation or dermal contact, and secondarily by injection or ingestion, if they are present in food or medicine.

On the other hand, nanoparticles may also concern the environment; since these particles have such a small dimension, they can be easily carried by air (i.e., airborne particles) or by water. For example, nano-ZnO and nano titanium dioxide (nano-TiO_2) contained in sunscreens may be released into the marine water when taking a bath.

Another study "The structure, composition, and dimensions of TiO_2 and ZnO nanomaterials in commercial sunscreens" by Lewicka et al. (2011)[18] investigated the structure of nano-ZnO pigments derived from actual sunscreen products. Sunscreens have ultraviolet blocking agents to attenuate damaging radiation before it can interact with skin. One of these blocking agents, thanks to its ability of scattering, reflecting, and absorbing UVA and UVB rays, is nano-ZnO. Spreading sunscreens with regular and abundant applications in order to avoid sunburns represent a great exposure to ZnO nanoparticles, and it is quite likely that during use or disposal they will also find their way into the environment and there they will interact with organisms. In Figure 1.3a and Figure 1.3b it is possible to see Scanning Electron Microscopy (SEM) and Transmission Electron Microscopy (TEM) images on nano-ZnO from sunscreen. These rod-shaped particles have an average dimensions of 80 nm in length and 37 nm in width.

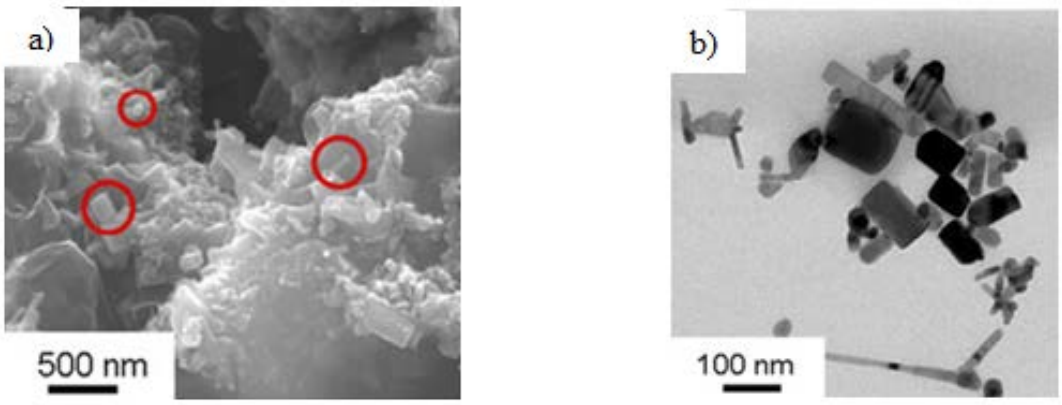

Figure 1.3. a) SEM image and b) TEM image of ZnO nanoparticles in sunscreens[18].

In a further study "Photochemical behavior of nanoscale TiO_2 and ZnO

sunscreen ingredients" by Lewicka et al. (2013)[19], the ability to produce reactive oxygen species (ROS) upon UV illumination of ZnO was investigated. ROS are radical, chemically-reactive molecules containing oxygen that can cause significant cell damage, including direct modification of nucleic acid bases and cell death. These particles may also affect ecosystems, inhibiting photosynthesis of phytoplankton. As a result, nano-ZnO generated a greater amount of ROS than TiO_2.

As such, due to the potential hazard posed by this nanoparticle and by its large presence in consumer products, it is essential to further inquire and estimate the release and toxicity of both industrial and commercially-available good's derived nano-ZnO toward the diatom *Thalassiosira pseudonana*. In particular, the present case study will focus on the differences between industrial-derived and sunscreen-derived zinc oxide nanoparticles, as well as the growth inhibition of *Thalassiosira pseudonana* induced by both types nanoparticles, as a function of their concentration and exposure time.

Chapter 2 - Literature review

Due to its properties, zinc oxide (as well as titanium dioxide) nanoparticles are often used as inorganic UV filter, as mentioned by Serpone et al. (2007)[20]: These metal oxide nanoparticles are known for their ability to absorb Ultraviolet A (wavelength ranging from 320 to 400 nm) and Ultraviolet B (wavelength ranging from 290 to 320 nm) radiation. Nano-ZnO is a physical filter: The radiation is blocked by means of reflecting and scattering sunlight.

Increasing awareness toward skin cancer (e.g., melanoma), attributed to the long exposure to intense sunlight[21], led to the implementation of sun safety practices, including the routine use of sunscreens. Indeed, sunscreens offer the best protection against UVA/UVB radiation skin damages[22]. The increase in the use of inorganic UV filters in sunscreen products is one of the latest trends, due to their effectiveness[20].

Coastal tourism recently became one of the fastest growing economic industries. As assessed in two studies by Sánchez-Quiles & Tovar-Sánchez (2014 and 2015), 763 million of tourists chose to travel to a coastal destination in 2004[21] , while 202 million of tourists chose to visit the Mediterranean Sea in 2013[23]. According to those studies, the number of tourists is estimated to continue to grow in the next years, and it is reasonable to assume that tourists will use sunscreens in order to prevent sunburns.

The study "The Safety of Nanosized Particles in Titanium Dioxide– and Zinc Oxide– based Sunscreens" by Newman et al. (2009)[24] reports that no significant skin penetration is expected from zinc oxide nanoparticles contained in sunscreen products; on the other hand it should be noted that:

- In vivo skin penetration tests are highly subjective to the tested species (e.g., rabbits, rats, pigs and humans) and to the compounds;
- In vitro studies were performed on intact skin, and therefore no information regarding traumatized or diseased skin (e.g., sunburned skin, eczema); and

- The studies were performed without UV exposure control.

The massive use of sunscreens represents a high risk of accumulation of metal oxide nanoparticles onto the skin and in the environment. In particular, these particles are likely to follow multiple pathways in the environment throughout their entire life cycle (i.e., nanoparticles synthesis, consumer product fabrication, consumer product usage, and consumer product disposal), as mentioned by Giokas et al. (2007)[25] and Sánchez-Quiles & Tovar-Sánchez (2015)[21]. Among those pathways it is important to mention:

- Industrial wastewater discharges from the production process;
- Landfill leachate from the residue in sunscreen packages;
- Sludge from wastewater treatment; and
- Wash off in water bodies during bathing activities.

The study "Ecotoxixity of Zinc Oxide Nanoparticles in the Marine Environment" by Yung et al. (2014)[26] reports the following modeled environmental concentrations of nano-ZnO, visible in Table 2.1. As a remark, the variability in the modeled concentrations indicates the use of different models and high uncertainties linked to those models.

The study "Sunscreen Products as Emerging Pollutants to Coastal Waters" by Tovar-Sánchez et al. (2013)[27], assessed that the majority of chemicals released from sunscreen products is concentrated in the surface microlayer of the water body, due to the greasy nature of sunscreens. Moreover, it was evaluated that the zinc oxide concentration in the surface microlayer of seawater varies from 1.0 to 3.3 μg/L throughout the day (peaking at midday), whereas the concentration in subsurface seawater is lower and more constant.

Surface water (ng/L)	Wastewater (µg/L)	Sludge (mg/kg)	Soil (µg/kg)	Sludge-treated soil (µg/kg)	Sediment (µg/kg)	Reference
76,000	/	2,172	/	3,194	/	Gottschalk et al. (2013)[28]
1-60	0.22-1.42	13.6-64.7	0.026-0.66	1.6-23.1	0.49-56	Gottschalk et al. (2009)[29] Gottschalk et al. (2010)[30]
0.1-100	1	10-100	1-100	10-100	100	Boxall et al. (2007)[31]

Table 2.1. Modeled concentrations of nano-ZnO in the environment.[26]

In light of that, despite the modeled and actual measured concentrations of zinc oxide nanoparticles in the environment, testing the growth inhibition induced by higher nanoparticle concentration is very important: Indeed, testing higher nano-ZnO concentrations will allow assessing the effects on the marine environment when the metal oxide is found in concentrated forms (i.e., sludge accumulation, presence of sediments), as well as bioaccumulation effects. Moreover, since the tourism industry is expected to be growing in the next decades, testing higher zinc oxide nanoparticle concentrations could be useful for future scenarios.

As soon as that the particles are released into water bodies, they are likely to interact with the aquatic environment. Several studies investigated the effects of zinc oxide nanoparticles toward the marine life; those studies are reported in the following paragraphs, starting with simple organisms (i.e., marine algae) and ending with more complex ones (i.e., zebrafishes, amphipods).

Regarding the possible effects of nano-ZnO on the marine environment, the study "Evaluation of zinc oxide nanoparticles toxicity on marine algae C*hlorella vulgaris* through flow cytometric, cytotoxicity and oxidative stress analysis" by Suman et al. (2015)[32] analyzed the toxicity of nano-ZnO and its effects on the marine algae C*hlorella Vulgaris*. Zinc oxide nanoparticles were synthesized in the laboratory, while the algae were purchased and cultured; for the experiments, an

initial amount of 4×10^5 cells were treated with 50 mg/L, 100 mg/L, 200 mg/L, and 300 mg/L each, for 24 and 72 hours. The results showed that the cell viability was correlated to both concentration of nano-ZnO and exposure time (Fig.2.1).

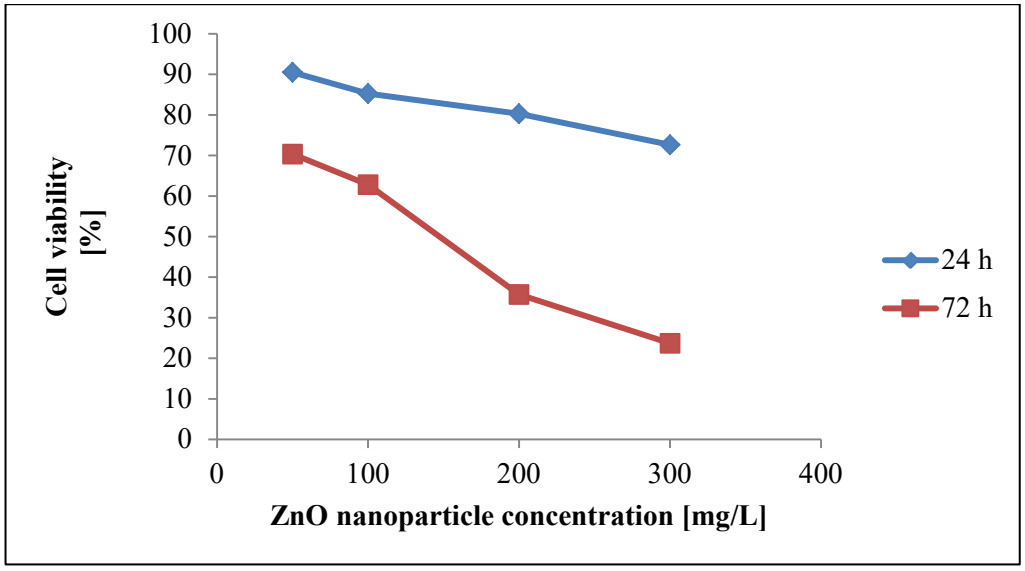

Figure 2.1. Cell viability (%) vs. nano-ZnO concentration[32].

Also, the cell integrity was altered. As can be seen, Figure 2.2a shows a control cell, without damages, while Figure 2.2b shows that after a 50 mg/L 72 h exposure, significant damages appear on the cell membrane. Finally, Figure 2.2c shows that after a 300 mg/L 72 hrs exposure, significant distortions appear to be present in the cell. Moreover, the integrity of the cell membrane was tested with propidium iodide (PI) stain: If the cell is not stained by PI, it means that the membrane is intact; otherwise, its integrity is compromised. As can be seen in Figure 2.3a, the control cells show no PI dye, whereas after a 300 mg/L 72 h exposure, the image shows PI dye entered the cell, due to membrane damages (Fig. 2.3b).

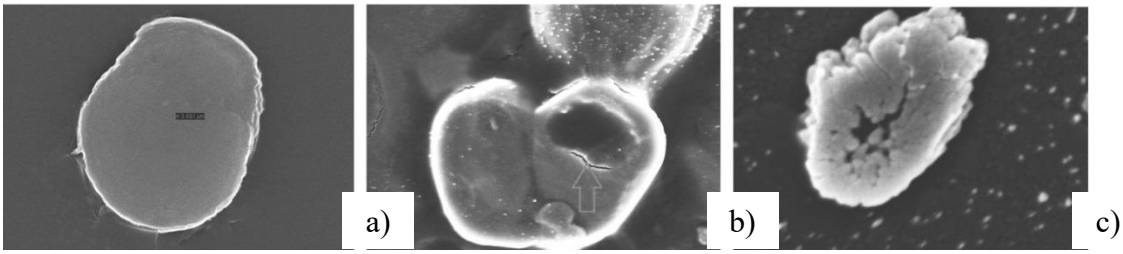

Figure 2.2. SEM image: a) control cell b) cell after 50 mg/L 72 h test c) cell after 300 mg/L 72 h test[32].

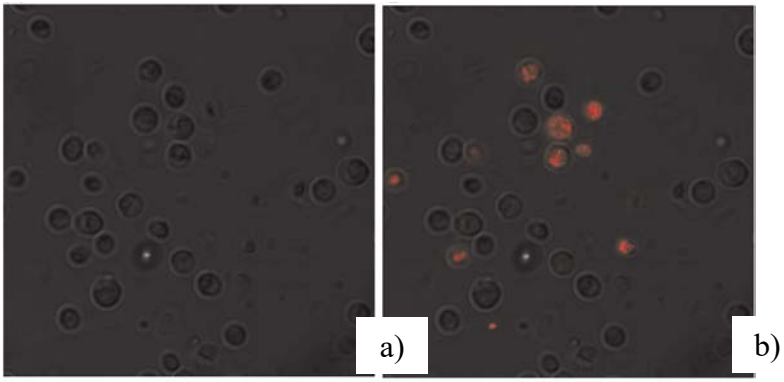

Figure 2.3. a) control cell, unstained b) cell after 300 mg/L 72 h test, stained[32].

Another study, "Toxic effects of ZnO nanoparticles toward marine algae *Dunaliella tertiolecta*" by Manzo et al. (2013)[33], analyzed the toxic effects of nano-ZnO on the marine algae *Dunaliella tertiolecta*. The experiments were conducted by preparing plates of 10 mL, with an algae concentration of 10^3 cells/mL, and loading them with a concentration of nano-ZnO of 100 mg/L (Fig.2.4), obtained from the dilution of 10 mg of dry powder of nano-ZnO into 100 mL of artificial seawater, and grown for four days. The final concentration in the samples was 10, 7.5, 5, 3, 1, 0.75, 0.5, and 0.1 mg Zn/L. The results showed that the growth rate was affected by the nanoparticle, at a 95% confidence interval (as bracketed in Table 2.2); NOEC stands for "No Observed Effect Concentration," LOEC stands for "Lowest Observed Effect Concentration," and EC50 and EC10 are, respectively, the Effective Concentration at 50 and 10 percent inhibition.

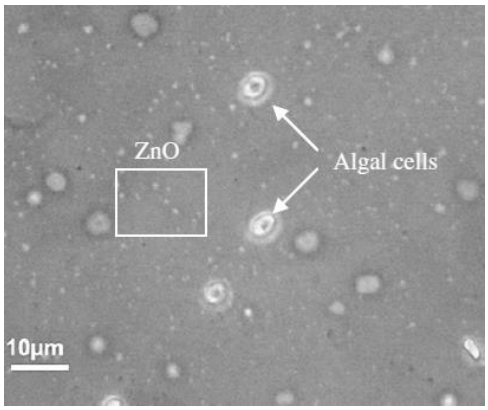

Figure 2.4. Phase contrast microscopy shows nano-ZnO and algal cells[33].

	NOEC [mg/L]	LOEC [mg/L]	EC50 [mg/L]	EC10 [mg/L]
Nano-ZnO	0.1	0.5	2.42 [0.97-2.87]	0.08 [0.06-0.14]

Table 2.2. NOEC, LOEC, EC50 and EC10 of nano-ZnO[33].

Table 2.3 shows the growth data and Figure 2.5 plots this data graphically, suggesting a correlation between the concentration and the survival rate of the cells of *Dunaliella tertiolecta*. As can be seen, increasing the concentration of the nanoparticle also increased the inhibition; that is to say, the growth rate decreased.

Concentration of ZnO [mg/L]	Growth rate
0	0.68 ± 0.02
0.1	0.65 ± 0.01
0.5	0.58 ± 0.02
0.75	0.57 ± 0.05
1	0.51 ± 0.06
3	0.44 ± 0.06
5	0.46 ± 0.05
7.5	0.2 ± 0.04
10	0.13 ± 0.05

Table 2.3. Growth rate vs. nano-ZnO concentration[33].

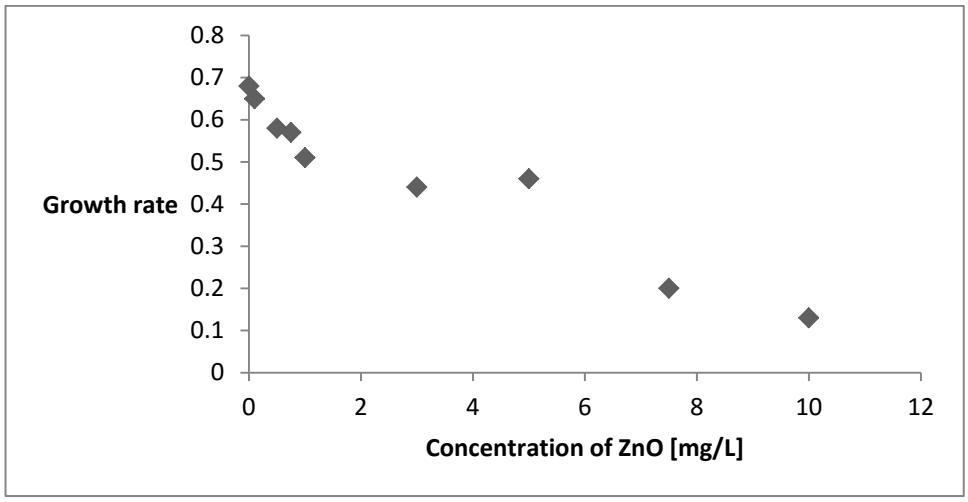

Figure 2.5. Growth rate vs. nano-ZnO concentration[33].

The study "Toxicity and Bioaccumulation of Nanomaterial in Aquatic Species" by Luo (2007)[34] evaluated the toxicity of nano-ZnO to the freshwater algae *Chlamydomonas reinhardtii* and to the freshwater water flea *Daphnia magna*. Since *Daphnia magna* naturally feeds on *Chlamydomonas reinhardtii*, three tests were

possible: Two direct toxicity tests, performed one on the algae and one on the water flea, and one bioaccumulation test performed on *Daphnia magna* which was fed on the nano-ZnO-long exposed *Chlamydomonas reinhardtii*. For the testing procedure, the algae strains were bought and then cultivated in the laboratory under controlled conditions. A fresh culture of water fleas was used for each experiment, and for every toxicity test 10 adults were used. Finally, nanoparticles were purchased and, for each test, added in concentrations of 1, 5, and 10 parts per million (ppm), respectively.

For what concerns the toxicity to *Chlamydomonas reinhardtii*, as can be seen in Figure 2.6, the toxicity of nano-ZnO is evident. When compared to both the absence of particles and the regular non-nano version of ZnO at 10 ppm, it is also possible to see that the number of cells is decreasing with the increment of nano-ZnO concentration. Moreover, it can be observed that acute toxicity (up to 48 hours of exposure) is lower than the long-term toxicity, measured after 20 days of growth. Further, the long-term test effects appear to be more evident and sharper, since the remaining population, in the case of 10 ppm, is approximately one third of the initial one.

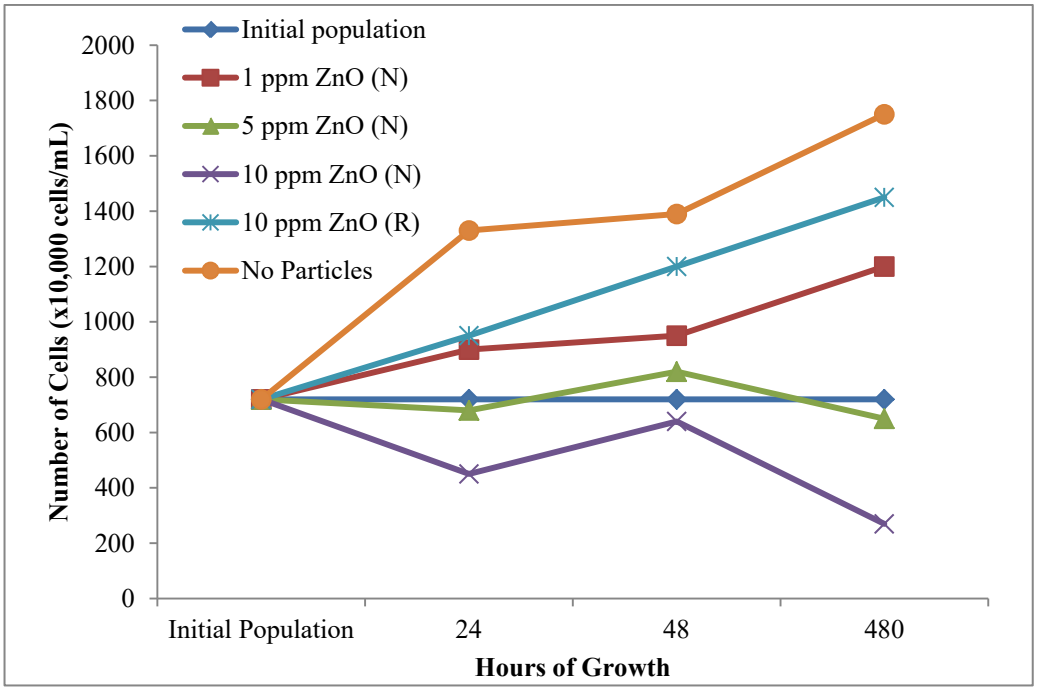

Figure 2.6. Toxicity test of *Chlamydomonas reinhardtii* at different nano-ZnO concentration[34].

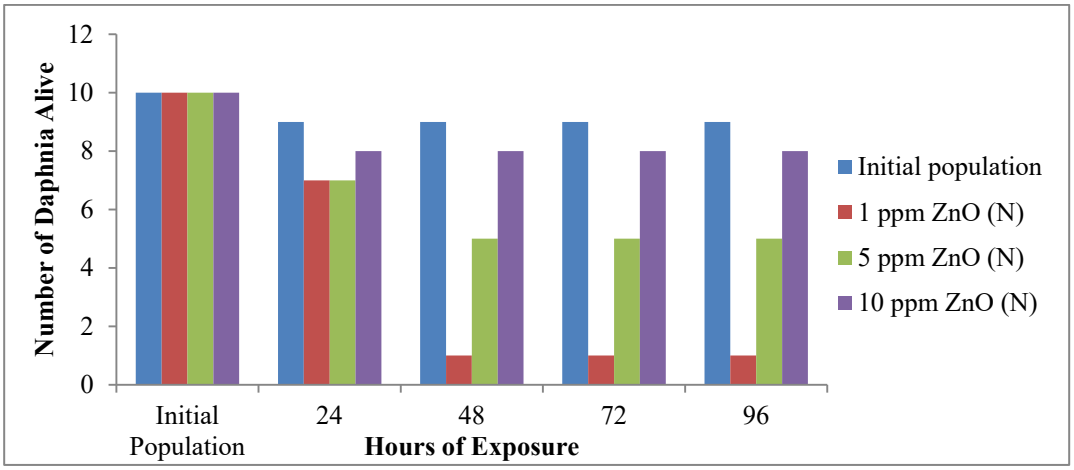

Figure 2.7. Direct toxicity test of *Daphnia magna*, at different nano-ZnO concentrations[34].

The direct toxicity test of *Daphnia magna*, whose results are presented in Figure 2.7, showed that, even for the water fleas, the nano-version of zinc oxide is more toxic, compared to the macro version. At 10 ppm, nano-ZnO appears to be very harmful to this water flea, while at lower concentrations it appears less toxic. On the other hand, it is important to notice that macro ZnO particles are more toxic to *Daphnia magna* than to *Chlamydomonas reinhardtii*. This may be due to the fact that the water flea has greater dimensions compared to those of the algae; therefore it is more likely that larger particles interact with larger organisms. Finally, concerning the bioaccumulation test, the indirect exposure of *Daphnia magna* to nano-ZnO produced a generic decrement in the water flea heartbeat, but the tendency is not always clear and this could be explained by some considerations:

- First, since this was an acute test ran for a short period of time, it does not take into account the possible further effects on subsequent generations;
- Second, the fleas were exposed to a very low amount of nano-ZnO; and
- Third, since *Daphnia magna* lives on stagnant water, it is likely that the nanoparticles settled and were no longer suspended.

In a study looking at more complex organisms, "Aquatic acute species sensitivity distributions of ZnO and CuO nanoparticles" by Adam et al. (2015)[35], the aquatic Species Sensitivity Distribution (SSD) (Fig.2.8) at the 5% Hazard

Concentrations (HC_5) of bacteria, protozoa, yeast, rotifera, algae, nematoda, crustacea, hexapoda, fish and amphibia species was evaluated. As a result, HC_5 was assessed to be 0.06 mgZn/L. To estimate it, both EC50 and LC50 (lethal concentration leading to death in 50% of the group) (Fig.2.9) were included, and those data were taken from past studies, in which the majority of nano-ZnO were purchased in powder form.

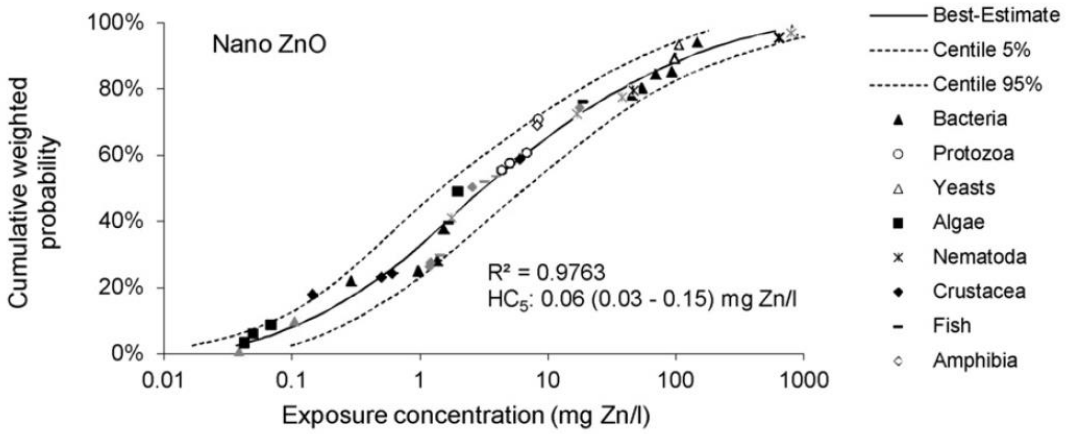

Figure 2.8. Aquatic SSD of nano-ZnO[35].

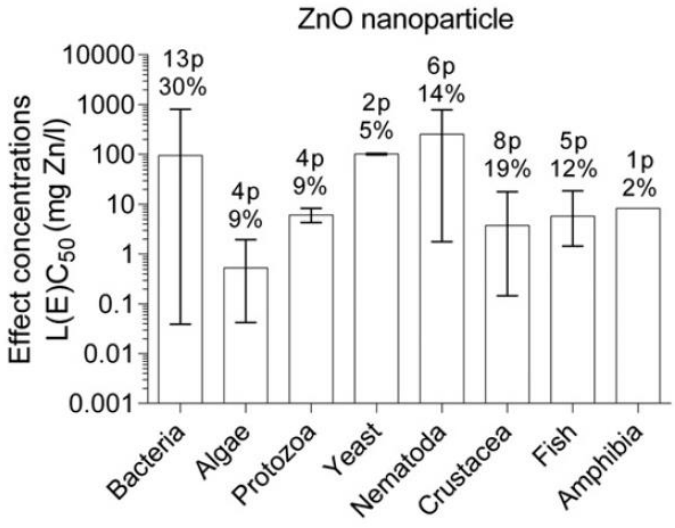

Figure 2.9. L(E)C50 values for different aquatic species[35].

As can be seen in Figure 2.9, algae appear to be the most susceptible aquatic organism to nano-ZnO, followed by crustacea. Moreover, an estimation of the

relationship between the aggregate size of the nano-ZnO and its toxicity to different aquatic species (Fig.2.10) was attempted; however this was possible only for fish and nematoda, but this could be due to the lack of data.

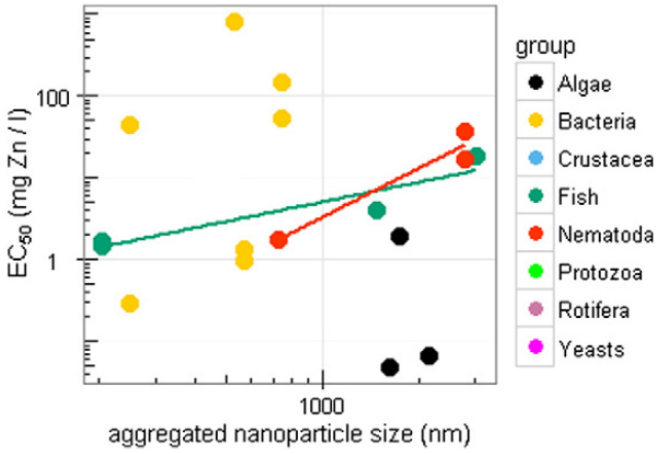

Figure 2.10. L(E)C50 vs. aggregate size for the different aquatic species[35].

In order to assess the risks associated to more complex but still not too specialized organisms, the study "Toxicity of zinc oxide nanoparticles to zebrafish embryo: a physicochemical study of toxicity mechanism" by Bai et al. (2010)[36] assessed the potential consequences on *Danio rerio* embryo exposed to polluting nano-ZnO, considering that this stage is the most delicate one during the life cycle of a fish. For the experiments, eggs were collected after spawning and nano-ZnO powder (particle size 30 nm) was purchased; the nanopowder was then added to the same medium used as hatchery water for the embryo in concentrations equal to 0, 1, 5, 10, 25, 50, and 100 mg/L (Fig.2.11a, Fig. 2.11b, and Fig. 2.11c). Among the initial 24 embryos, 20 were exposed to nano-ZnO and 4 were kept as a control sample. The embryos were then checked at 8, 24, 32, and from 48 to 96 Hours Post Fertilization (HPF).

As can be seen in Figure 2.12a, by increasing the concentration of polluting nano-ZnO, the hatching rate at 96 HPF consequently decreases, reaching the condition of unhatched eggs with concentrations equal to 25, 50, and 100 mg/L. Looking at figure 2.12b, it is possible to see the cumulative hatching vs. time of the embryos subjected to different concentrations: For instance, a concentration as low as 1 mg/L produces a slight effect, compared to the control samples, whereas

increasing the concentration it can be noticed that the zebrafish embryo hatching was delayed parallel to the increment in concentration of ZnO.

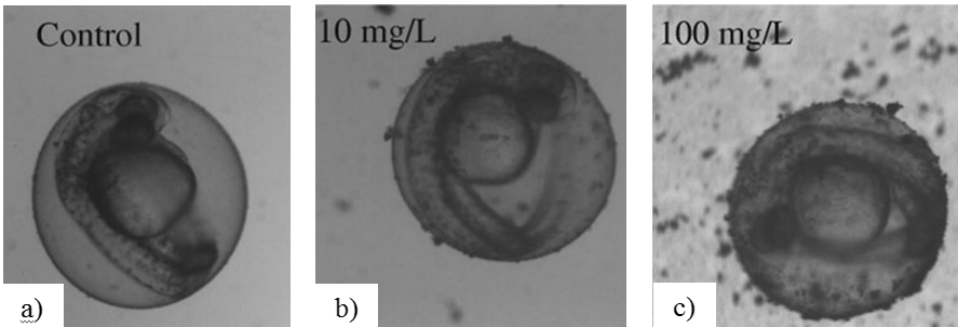

Figure 2.11. Zebrafish embryos: a) control; b) 10 mg/L exposition; c) 100 mg/L exposition[36].

The median hatching time (HT50) was then calculated, as can be seen in Table 2.4. For concentrations greater than 10 mg/L the time was not measured due to low hatching rate or no hatching.

	Control	1 mg/L	5 mg/L	≥ 10 mg/L
HT50 [h]	52.4 ± 1.2	52.7 ± 0.7	71.1 ± 14.8	/

Table 2.4. Median hatching time (HT50) at different concentrations[36].

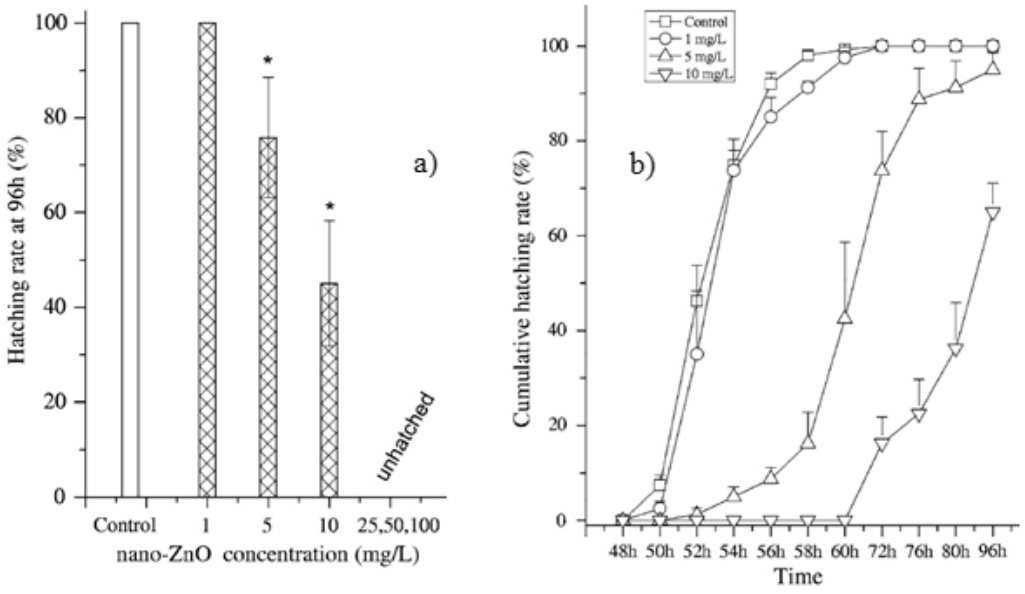

Figure 2.12. a) Hatching rate after 96 HPF;)Cumulative hatching from 48 to 96 HPF[36].

The mortalities among the embryos at 96 HPF was estimated to be 28.3 ± 14.5 % for 50 mg/L exposure and 65.0 ± 8.9 % for 100 mg/L. Moreover, it was possible to

measure variations in the length of the embryos by observing an overall shortening and a significant tail deformation as seen in Figure 2.13a and Figure 2.13b.

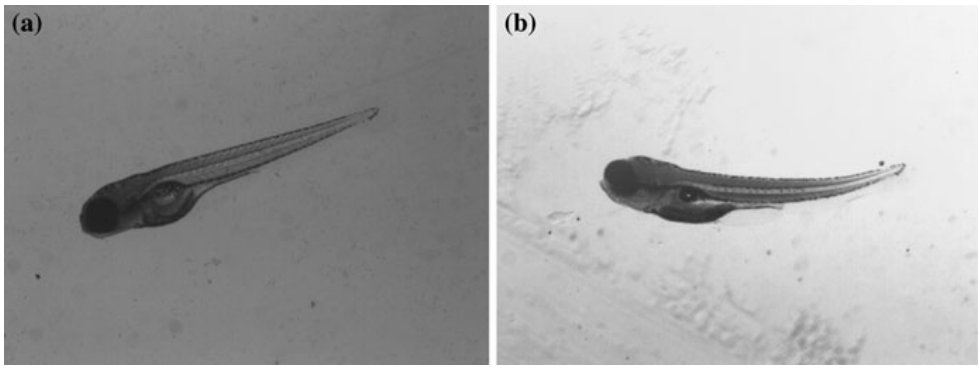

Figure 2.13. Comparison between a) control embryo and b) tail-malformed embryo.[36]

Therefore, the effects of nano-ZnO of zebrafish embryo include death, delayed hatching, reduced body length, and significant tail malformations.

Finally, to investigate the toxicity of nano-ZnO among more complex organisms, the study "Accumulation and toxicity of metal oxide nanoparticles in a soft-sediment estuarine amphipod" by Hanna et al. (2013)[37] tried to evaluate the effects that settlings of engineered nanoparticles, such as nano-ZnO, in estuary and marine sediments could have on *Leptocheirus plumulosus*, an amphipod that filters and feeds deposits. It is logical that, due to aggregation, nanoparticles will settle in sediments, reaching a locally high concentration of pollutants. First, the solubility of nano-ZnO was tested and the results showed that this nanoparticle dissolved rapidly in water; then, the proper toxicity tests were performed for 10 days, with adult amphipods and mixing sediments in concentrations of 0, 500, 1000, 1500, and 2000 μg/g of dry weight. As a result, the accumulation of nano-ZnO in live amphipods was less than 600 μg Zn/g, but, due to low survival, this was measured only for concentrations ranging from 0 to 1000 μg/g. Moreover, the estimated median lethal concentration LC50 after 10 days of exposure to nano-ZnO was assessed to be equal to 763 ± 64 μg g^{-1} and the mortality rate increased parallel to the increment of concentration of pollutant. The overall result of the study is that nano-ZnO is toxic to *Leptocheirus plumulosus*, and this toxicity can be due to its exposure to ions.

As such, algae play a very important role in aquatic systems as producers in the food chain and as oxygen providers in an ecosystem. For the present case study, the

diatom *Thalassiosira pseudonana* was chosen to perform growth inhibition tests. The diatom is a marine algae that can grow in both seawater and freshwater[38] and presents a worldwide marine distribution[39]; its DNA was sequenced[40] and has already been used in many toxicology experiments[41,42]. *Thalassiosira pseudonana* was selected among other aquatic organisms, for its role and presence in the marine ecosystem and for the relevant outcomes of previous case studies: The diatom can be used as an indicator of marine pollution.

As reported by Armbrust et al. (2004), in the study "The genome of the diatom Thalassiosira pseudonana: ecology, evolution, and metabolism"[40], the diatom presents a hydrated silicon dioxide (i.e., silica) frustule[43]. The frustule is a exoskeleton consisting of highly organized nanoparticles[43]; in Figure 2.14 it is possible to see a Scanning Electron Microscopy image of the silica-based frustule of *Thalassiosira Pseudonana*.

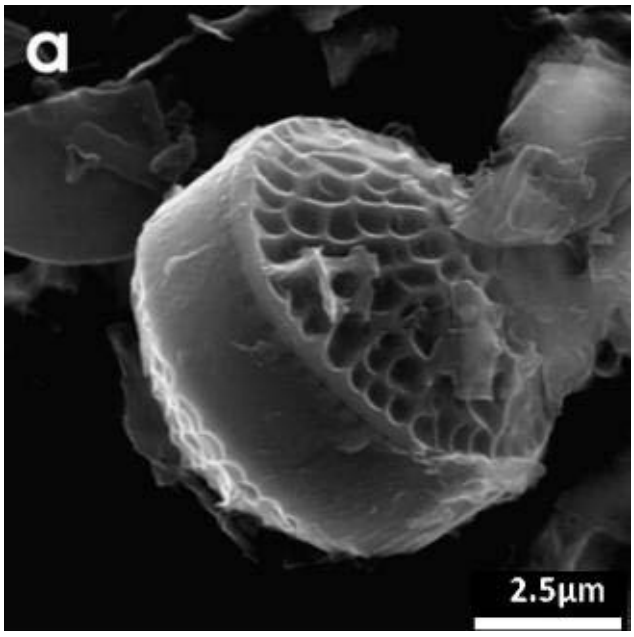

Figure 2.14. Frusutle of Thalassiosira Pseudonana.[43]

Concerning toxicity, several studies investigated the relationship between silica-based frustules and the presence of zinc oxide in the aqueous media. In particular, Ellwood and Hunter[44] assessed that the higher the concentration of zinc ion Zn^{2+} in the aqueous media, the higher the cellular uptake; on the other hand, just a small quantity of zinc uptake by the diatom is found in the frustules. Other studies[41,45]

reported that the toxicity of ZnO toward *Thalassiosira Pseudonana* might be linked to zinc ions Zn^{2+} attaching to the diatom's surface. Finally, Fisher et al. (1981)[46] reports that zinc ion Zn^{2+} might interfere with frustule formation.

Thus, understanding the potential issue represented by nano-ZnO, extracted from commercially available products like sunscreen to the survival rate of *Thalassiosira pseudonana* will provide invaluable information regarding the toxicity of the aforementioned nanoparticles.

The fundamental hypothesizes of the present case study can be then summarized:

- Do zinc oxide nanoparticles derived from commercially available products (i.e., sunscreens) behave similarly to industrial-derived ones?
- What is the growth inhibition developed from the intoxication of a simple food chain producer, like *Thalassiosira pseudonana*?

Moreover, the uniqueness of this research is represented by sunscreen-derived nanoparticles. At the present date, very few nanotoxicologial studies concerning self-extracted nanoparticles were conducted. The present case study introduces sunscreen-derived zinc oxide nanoparticles and compares the growth inhibition promoted by sunscreen-derived and industrial-derived, as a function of their concentration and exposure time.

The present study aims to unveil the possible issues posed by zinc oxide nanoparticles, present in sunscreen products, to the simple, food chain producer, aquatic organism.

Chapter 3 - Industrial nano-ZnO

The aim of the following experiments is testing the toxicity of industrial-derived zinc oxide nanoparticles to the diatom *Thalassiosira pseudonana*. The toxicity to the algal cells was expressed in terms of growth inhibition, which was estimated by the difference in the absorbance of the specimens with respect to the control sample. The experiments were performed in the Environmental Engineering Laboratory of the University of Miami.

3.1 Technical equipment

3.1.1 Beckman Coulter DU 720 Spectrophotometer

A DU 720 UV/Vis Spectrophotometer[47] (Beckman Coulter, DU® 720, Pasadena, CA), visible in Figure 3.1 is used in order to measure the absorbance (i.e., the amount of light absorbed by the sample). Its wavelength range is 190-1100 nm, while the absorbance can be measured with a precision of 0.001 Abs. Prior to running the experiment and measuring the absorbance of a sample, is it necessary to select an appropriate wavelength range and scan a blank sample.

Figure 3.1. DU 720 UV/Vis Spectrophotometer[47] (Beckman Coulter, DU® 720, Pasadena, CA).

3.1.2 Zetasizer Nano ZS90

A Zetasizer Nano ZS90[48] (Malvern Instruments, UK), visible in Figure 3.2, is used to measure both the size of particles in an aqueous media and the zeta potential of the colloid. Particle size can be measured for particles having a diameter in the

range of 0.3nm to 5.0 microns, while zeta potential can be measured for particles having a diameter in the range of 3.8 nm to 100 microns, with an accuracy of 0.12 µm cm/Vs. Measurements can be taken by placing the aqueous media in the appropriate cuvette; the specific cuvette for the zeta potential test can be seen in Figure 3.3.

Figure 3.2. Zetasizer Nano ZS90[48] (Malvern Instruments, UK).

Figure 3.314. Cuvette for zeta potential test[48].

3.1.3 Verilux VT 10 - 5000 lux

The Verilux VT 10 - 5000 lux[49] (Verilux, VT) (Figure 3.4) is used in combination with an incubator in order to provide an optimal environment for the growth of *Thalassiosira pseudonana*. The lamp has a timer which allows dark:light cycles (12h:12h). Dark:light cycles are essential to the diatom due to its photosynthetic nature.

Figure 3.4. Verilux VT 10 - 5000 lux[49] (Verilux, VY).

3.1.4 Orion™ pH meter and glass electrode

The pH meter Orion™ 720Aplus [50](Thermo Fisher Scientific, MA) visible in Figure 3.5, together with the glass electrode Orion™ 8156BNUWP[50] (Thermo Fisher Scientific, MA), visible in Figure 3.6, was used on order to assess the solution's pH.

Figure 3.5. Orion™ 720Aplus[50].

Figure 3.6. Orion^{TM} 8156BNUWP[50].

3.2 Manufacture of artificial seawater and f/2 medium

The diatom needs artificial seawater and f/2 medium in order to survive in the laboratory. Artificial seawater and f/2 medium were prepared in the laboratory according to Guillard et al. (1962)[51] and Keller et al. (1988)[52], using the following protocol.

Autoclaved artificial seawater is prepared dissolving the following amounts (Zhang et al, 2013.) in 1 liter of ultrapure water (18.2 MΩ) produced with a three-stage Millipore Milli-Q plus 185 purification system (Millipore, Billerica, MA).

- 27.72 g NaCl (>99.0% purity, Fisher Scientific, Fair Lawn, NJ);
- 0.67 g KCl (99.7% purity, Sigma-Aldrich, St. Louis, MO);
- 1.03 g $CaCl_2$ (>99.0% purity, Sigma-Aldrich, St. Louis, MO);
- 4.66 g $MgCl_2$ (>99.0% purity, BDH Chemicals, Radnor, PA);
- 3.07 g MgSO4 (>99.5% purity, Sigma-Aldrich, St. Louis, MO); and
- 0.18 g $NaHCO_3$ (99.9% purity, Mallinckrodt, Paris, KY).

Artificial seawater was then adjusted to a pH of 8.0 by means of adding 1 M NaOH or HCl; the pH was monitored with a pH meter (Orion™, 720Aplus) with a glass electrode (Orion™, 8156BNUWP).

The f/2 medium is designed for growing diatoms. The concentration of the original formulation, termed "f Medium" by Guillard et al. (1962)[51], has been reduced by half. The following components, presented in Table 3.1, are added to 950 mL of artificial seawater, then the final volume is brought to 1 liter with autoclaved artificial seawater.

Component	Stock solution	Quantity	Concentration
$NaNo_3$	75 g/L	1 mL	8.82 x 10^{-4} M
NaH_2PO_4H2O	5 g/L	1 mL	3.62 x 10^{-5} M
Trace metal solution	-	1 mL	-
Vitamin solution	-	0.5 mL	-

Table 3.1. f/2 medium composition.

3.2.1 Manufacture of f/2 Trace Metal Solution

The following components, presented in Table 3.2, are added to 950 mL of H_2O, then the final volume is brought to 1 liter with autoclaved artificial seawater.

Component	Stock solution	Quantity	Concentration
$FeCl_3$ 6H2O	-	3.15 g	1.17 x 10^{-5} M
Na_2 EDTA 2H2O	-	4.36 g	1.17 x 10^{-5} M
$CuSO_4$ $5H_2O$	9.8 g/L H_2O	1 mL	3.93 x 10^{-8} M
Na_2MoO_4 $2H_2O$	6.3 g/L H_2O	1 mL	2.60 x 10^{-8} M
$ZnSO_4$ $7H_2O$	22.0 g/L H_2O	1 mL	7.65 x 10^{-8} M
$CoCl_2$ $6H_2O$	10.0 g/L H_2O	1 mL	4.20 x 10^{-8} M
$MnCl_2$ $4H_2O$	180.0 g/L H_2O	1 mL	9.10 x 10^{-7} M

Table 3.2. f/2 Trace Metal Solution composition.

3.2.2 Manufacture of f/2 Vitamin Solution

The following components, presented in Table 3.3, are added to 950 mL of H_2O, then the final volume is brought to 1 liter with autoclaved artificial seawater.

Component	Stock solution	Quantity	Concentration
Thiamine HCl (vit. B1)	-	200 mg	2.96 x 10^{-7} M
Biotin (vit. H)	1.0 g/L H_2O	1 mL	2.05 x 10^{-9} M
Cyanocobalamin (vit B12)	1.0 g/L H_2O	1 mL	3.69 x 10^{-10} M

Table 3.3. f/2 Vitamin Solution composition.

3.3 Nanoparticles

Commercial ZnO nanopowder (>97% purity, <50 nm ± 5 nm nominal size, >10.8 m^2/g surface area, data from vendor) was purchased from Sigma-Aldrich[53] (St. Louis, MO). The toxic effects of nano-ZnO were investigated by suspending 1, 10, and 50 mg of ZnO nanoparticles in 1 L of artificial seawater f/2 medium.

3.4 Diatom culture

Thalassiosira pseudonana cells were purchased from Bigelow Laboratory for Ocean Sciences (CCMP 1335[54]). The culture of *Thalassiosira pseudonana* was obtained by adding artificial seawater f/2 medium to the originally purchased culture. Then the culture was incubated at a constant temperature of 26°C, with 12h:12h (dark:light) cycles maintained with Verilux VT 10 (5000 lux, white light).

3.5 Experimental setup

3.5.1 Detection of *Thalassiosira pseudonana* absorbance wavelength

In order to estimate the growth inhibition induced by industrial nano-ZnO toward the marine diatom *Thalassiosira pseudonana*, several absorbance tests were performed. The aim of the experiment is to find a relationship between the absorbance, measured with the spectrophotometer, and the algae concentration in the samples. This indirect measurement of the growth inhibition was chosen due to the difficulties associated with direct measurements.

The issue associated with this type of indirect measurement was finding the wavelength corresponding to the algae's peak in the red band. Tests were performed after a literature review, in order to narrow the broad spectrum of all possible wavelengths. Three studies involving spectrophotometer tests were considered.

The first study is "UV effects on photosynthesis, growth and acclimation of an estuarine diatom and cryptomonad" by Litchman & Neale (2005)[55]. The sensitivity of photosynthesis and acclimation to UV of *Thalassiosira pseudonana* were tested and UV spectrum analysis, comparing the three different expositions to light, were performed. The results of the UV spectrum analysis are shown in Figure 3.7.

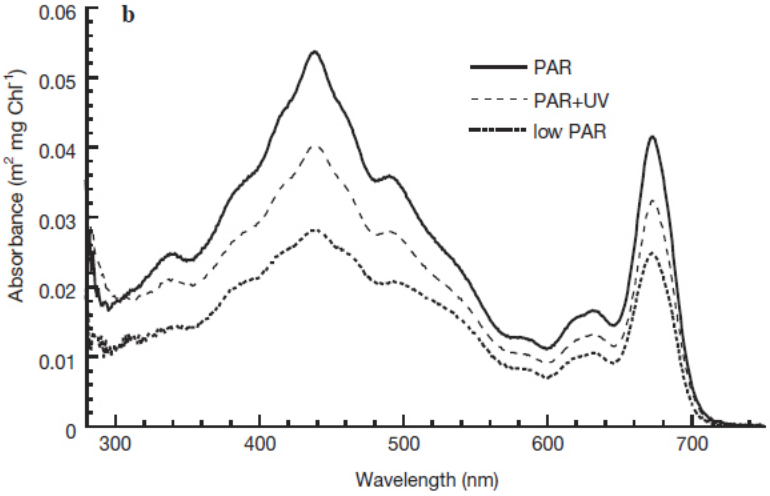

Figure 3.7. Absorbance vs. wavelength[55].

Another study, "The effect of nitrogen limitation on the absorption and scattering properties of the marine diatom *Thalassiosira pseudonana*" by Reynolds et al. (1997)[56], investigates the optical properties of *Thalassiosira pseudonana* in nitrate-limited semicontinuous cultures at different growth rates, and indicates λ = 673 nm as the algae's absorption red peak, as can be seen in Figure 3.8.

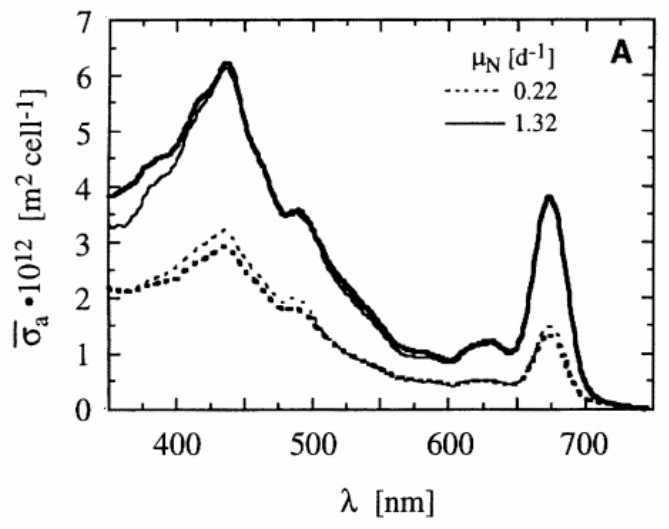

Figure 3.8. Absorbance vs. wavelength[56].

The third study, "Reflectance spectroscopy of marine phytoplankton. Part 1. Optical properties as related to age and growth rate" by Kiefer et al. (1979)[57], investigates the optical properties of two different algae; one of the algae included in

the study is *Thalassiosira pseudonana*. The research indicates that the red peak associated to this diatom is λ=673 nm, as can be observed in Figure 3.9.

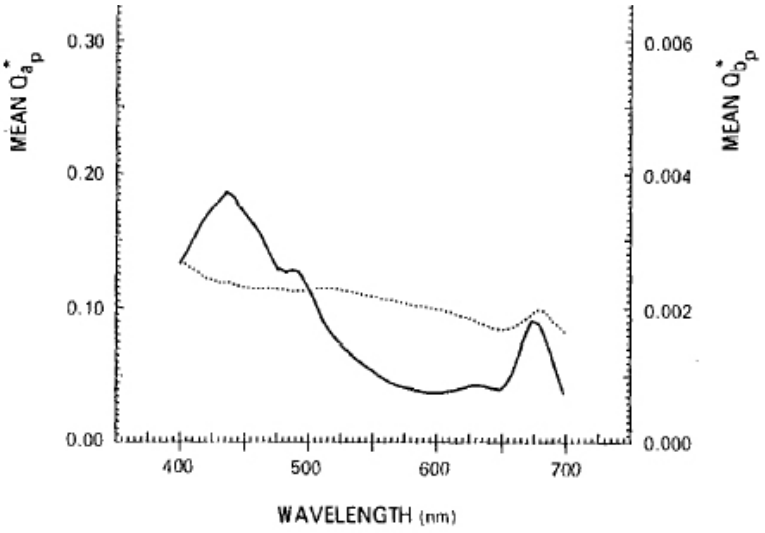

Figure 3.9. Absorbance vs. wavelength[57].

After having narrowed the list of all possible wavelengths, tests were performed in order to assess the right wavelength of *Thalassiosira pseudonana*. First, the absorbance of a sample of *Thalassiosira pseudonana* in artificial seawater (1:1) was analyzed, and other measurements were taken after performing serial dilutions, halving the diatom concentration at each step. The sample corresponding to the dilution 1:256 represents the detection limit of the spectrophotometer, since the absorbance measured was 0.001. As can be seen in Table 3.4, a wide range of wavelengths were tested, and measurements assessed that the peak of absorption of *Thalassiosira pseudonana* occurred at a wavelength corresponding to 674 nm. The relationship between the absorbance of *Thalassiosira pseudonana* and its concentration in artificial seawater, for a wavelength of 674 nm can be seen in Figure 3.10. This value was used to analyze the changes in the absorbance of poisoned diatom cells in next experiments.

Wavelength [nm]		672	673	674	675	676
Concentration of *T. pseudonana*	1:1	0.150	0.150	0.151	0.150	0.150
	1:2	0.079	0.079	0.079	0.079	0.079
	1:4	0.039	0.039	0.040	0.039	0.039
	1:8	0.020	0.020	0.020	0.020	0.020
	1:16	0.013	0.013	0.013	0.013	0.013
	1:32	0.005	0.005	0.005	0.005	0.005
	1:64	0.003	0.003	0.003	0.003	0.003
	1:128	0.002	0.002	0.002	0.002	0.002
	1:256	0.001	0.001	0.001	0.001	0.001

Table 3.4. Absorbance of *Thalassiosira pseudonana* in Artificial Seawater as a function of concentration, for different wavelenghts.

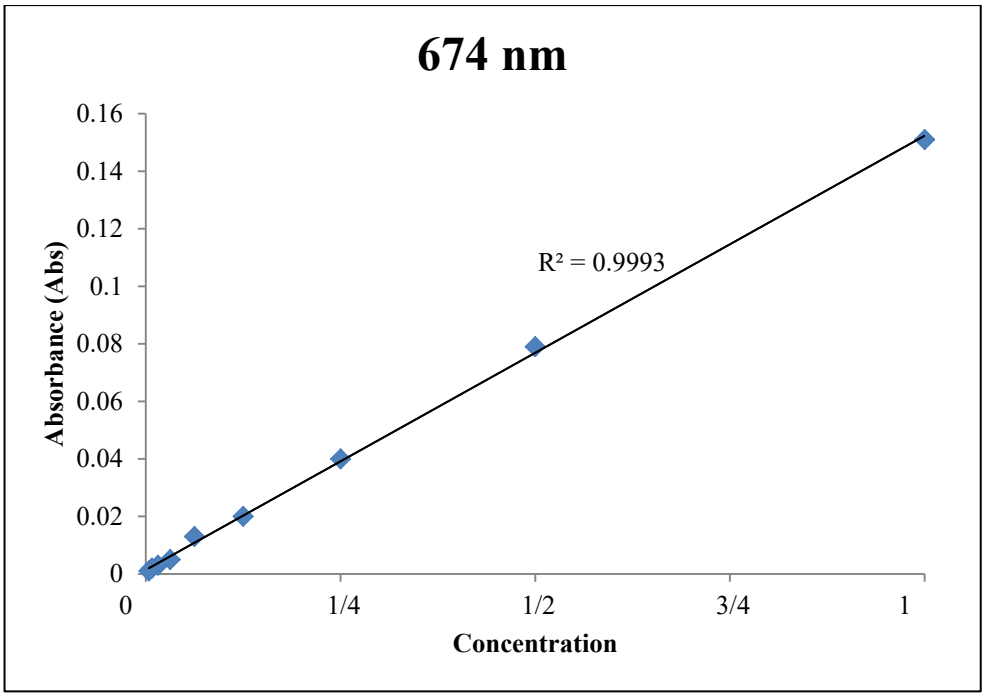

Figure 3.10. Absorbance vs. Concentration at peak wavelength of *Thalassiosira pseudonana.*

3.5.2 Calibration of nano-ZnO absorbance

Several absorbance tests were performed, in order to understand whether the zinc oxide nanoparticle's wavelength peak interferes with the absorbance measurements of *Thalassiosira pseudonana*. The wavelength peak of nano-ZnO was found equal to 395 nm and was confirmed by measuring six concentrations of nano-ZnO (Table 3.5) with a wavelength range of 350-400 nm.

Concentration ZnO (mg/L)	Absorbance (abs)
100	0.392
50	0.186
25	0.074
12.5	0.035
6.25	0.014
3.125	0.004

Table 3.5. Inhibition (%) as a function of exposure time, industrial ZnO, 10 mg/L.

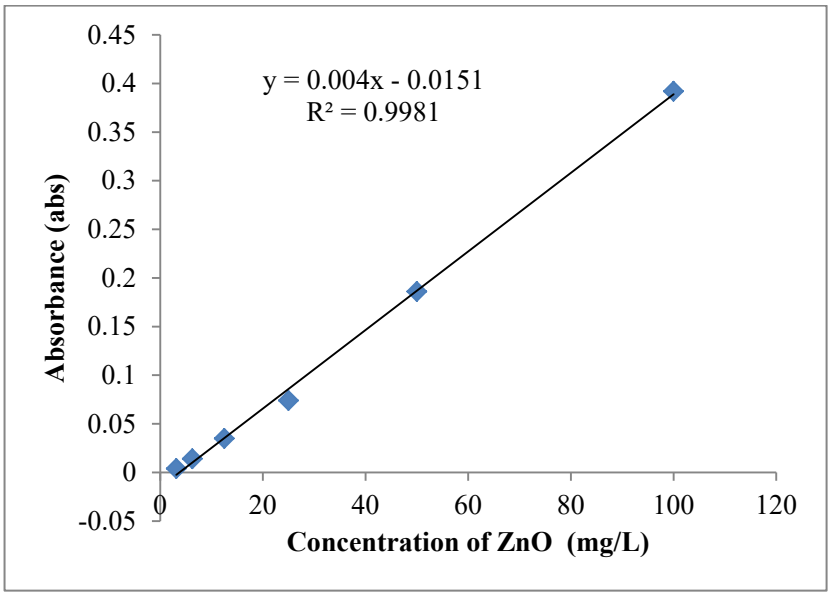

Figure 3.11. Absorbance vs. Concentration of nano-ZnO.

The relationship between the absorbance of nano-ZnO and its concentration can be seen in Figure 3.11.

3.5.3 Inhibition (%) as a function of exposure time

For the triplicate experiment, 15 mL of nanoparticle suspension were inoculated in 15 mL of diatom culture and placed in a 50 mL Petri dish, gently mixing it afterwards. For industrial nano-ZnO, two concentrations were tested: 10 and 50 mg/L. Control samples consisted in 15 mL of artificial seawater f/2 medium diluted into 15 mL of algae mass culture. Absorbance measurements were repeated at fixed time steps (5, 12, 24, 48, 72, and 96 hours after inoculation).

3.5.4 Effect of ZnO concentrations at fixed exposure time

For the two triplicate experiments, 15 mL of nanoparticle suspension were inoculated in 15 mL of diatom culture and placed in a 50 mL Petri dish, gently mixing it afterwards. For industrial nano-ZnO, three concentrations were tested: 1, 10, and 50 mg/L. Control samples consisted in 15 mL of artificial seawater f/2 medium into 15 mL of algae mass culture. The absorbance was measured (the latter with Beckman Coulter DU 720 spectrophotometer) and samples were incubated. Then, absorbance measurements were repeated after 48 hours.

3.6 Results

3.6.1 Zinc Oxide dissolution

Prior to performing the growth inhibition experiments, the dissolution (%) of two concentrations of ZnO nanoparticles (10 mg/L and 50 mg/L) as a function of the pH of the aqueous media was assessed by means of Visual MINTEQ, as can be seen in Figure 3.12, while Figure 3.13 plots the amount of dissolved zinc ion Zn^{2+} (expressed in mg/L) as a function of the pH.

The information regarding dissolution (%) and pH was used in order to estimate the amount of dissolved zinc ion in the aqueous media as a function of the exposure time. The pH of *Thalassiosira pseudonana* exposed to industrial-derived nano-ZnO (50 mg/L), measured at 0 and 48 hours after inoculation, had a constant value of 8.5 (Spisni and Seo et al., 2016 submitted[58]).

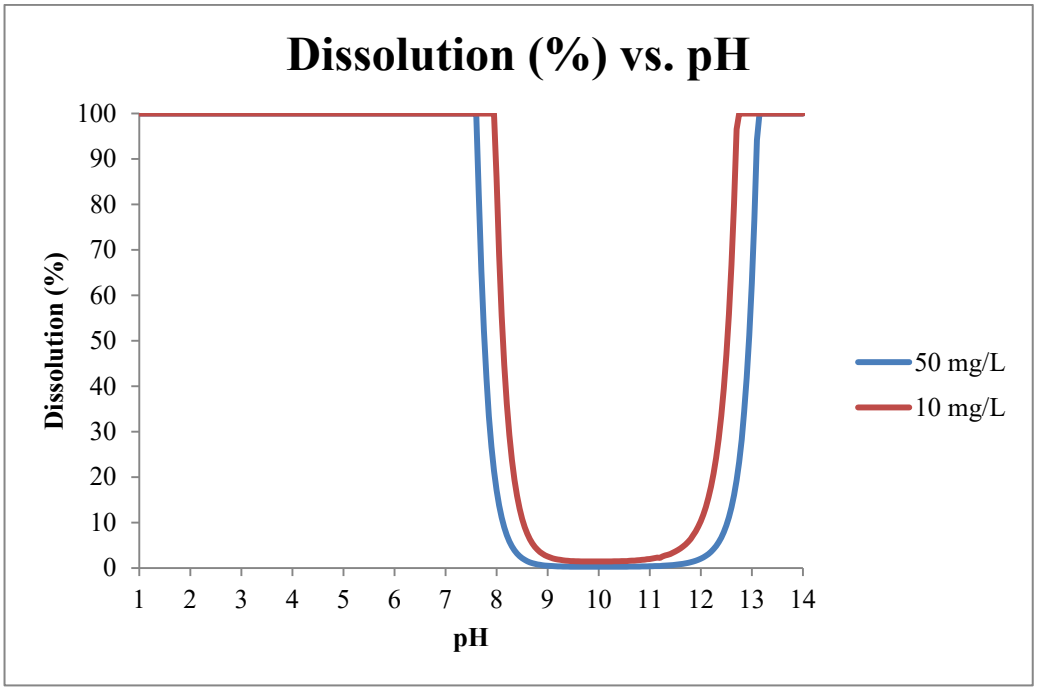

Figure 3.12. Dissolution (%) of zinc oxide vs. pH.

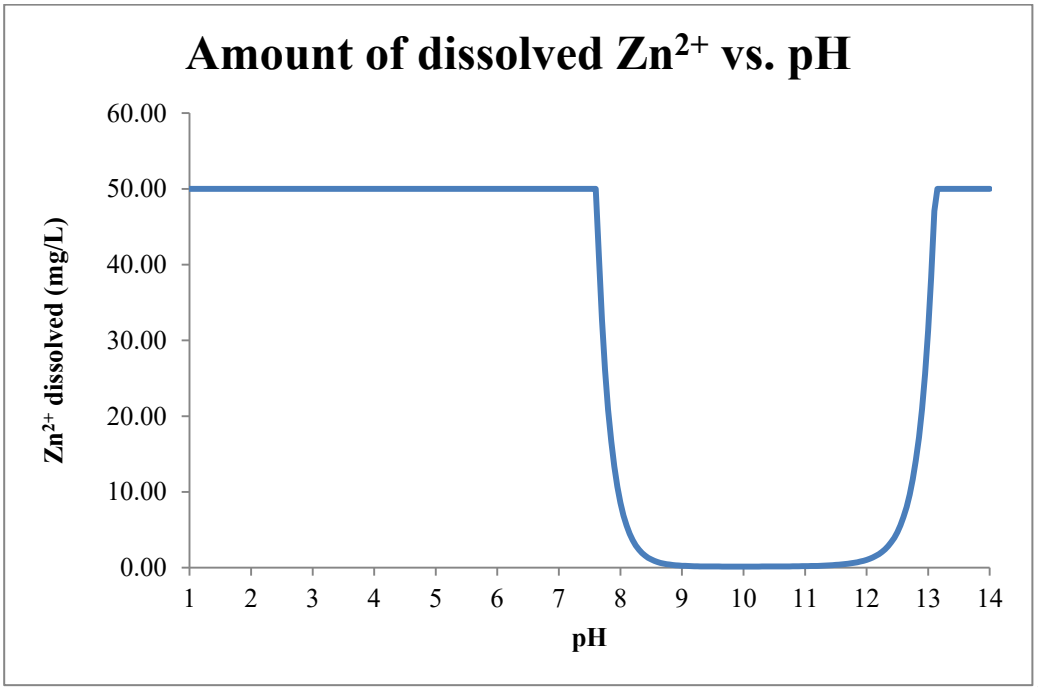

Figure 3.13. Zn^{2+} dissolved (mg/L) vs. pH.

3.6.2 Particle size and zeta potential

The particle size of industrial-derived zinc oxide nanoparticles, as mentioned in Spisni and Seo et al. (2016, submitted)[58] was assessed by means of X-Ray Diffraction (XRD) analysis. The measurement indicates that industrial-derived zinc oxide nanoparticles have a diameter equal to 24 nm.

A Zetasizer Nano ZS90 (Malvern Instrument, UK) was used in order to measure the particle size and the zeta potential of *Thalassiosira pseudonana* exposed to industrial-derived nano-ZnO (50 mg/L). The measurements, taken at 0 and 48 hours after inoculation, showed that the particle size slightly increased from 1549 nm to 1574 nm, while the zeta potential decreased from -9.0 mV to -8.5 mV (Spisni and Seo et al., 2016 submitted[58]).

3.6.3 Inhibition (%) as a function of exposure time

The results of the experiments are presented in the following tables. In rows 3 to 5 it is possible to see the absorbance values of the three control samples, while in row 6 it is possible to see their average. Then, in rows 9 to 11 it is possible to see the absorbance values of the three ZnO samples (10 mg/L in Table 3.6 and 50 mg/L in Table 3.7), while in row 12 it is possible to see their average.

The inhibition (%) of *Thalassiosira pseudonana*, reported in row 15, was computed using the following formula, according to the study "Growth Inhibition and Induction of Apoptosis in SHG-44 Glioma Cells by Chinese Medicine Formula 'Pingliu Keli'" by Cao et al. (2011)[59]:

$$\%\ \text{inhibition (t)} = 100 - 100 * \frac{\text{average absorbance ZnO (t)}}{\text{average absorbance control (t)}}$$

Several statistical analysis were conducted:

- The standard deviation, σ, measuring the dispersion of a set of data, visible in rows 7, 13, and 16, is computed according to the following, where n = 3 and $\bar{x}$ is the average of the three samples:

$$\sigma=\sqrt{\frac{\sum(x-\bar{x})^2}{(n-1)}}$$

- The Standard Error of the Mean, (i.e., SEM), measuring the precision of the mean, visible in rows 8, 14, and 17, is computed according to the following:

$$SEM=\frac{\sigma}{\sqrt{n}}$$

- The Student's *t*-test (Two samples assuming equal variance), with the purpose of determining whether two data sets are significantly different from each other (control samples vs. nano-ZnO samples): Statistical significance ($p < 0.05$) was found for each set of data with $t > 24$ hours.

The results of the experiments can be seen in Figure 3.14, and Figure 3.15.

concentration	10	mg/L					
Time (h)	0	5	12	24	48	72	96
Absorbance control 1	0.0130	0.0110	0.0120	0.0460	0.0720	0.0930	0.1020
Absorbance control 2	0.0170	0.0120	0.0130	0.0430	0.0680	0.0910	0.1050
Absorbance control 3	0.0140	0.0120	0.0150	0.0470	0.0690	0.0890	0.1070
Average absorbance of controls	0.0147	0.0117	0.0133	0.0453	0.0697	0.0910	0.1047
ST DEV	0.0021	0.0006	0.0015	0.0021	0.0021	0.0020	0.0025
SEM	0.0012	0.0003	0.0009	0.0012	0.0012	0.0012	0.0015
Absorbance sample 1	0.0130	0.0100	0.0130	0.0390	0.0470	0.0560	0.0600
Absorbance sample 2	0.0140	0.0110	0.0130	0.0370	0.0460	0.0550	0.0590
Absorbance sample 3	0.0150	0.0110	0.0120	0.0360	0.0450	0.0560	0.0610
Average absorbance of samples	0.0140	0.0107	0.0127	0.0373	0.0460	0.0557	0.0600
ST DEV	0.0010	0.0006	0.0006	0.0015	0.0010	0.0006	0.0010
SEM	0.0006	0.0003	0.0003	0.0009	0.0006	0.0003	0.0006
% inhibition	0.000	8.571	5.000	17.647	33.971	38.828	42.675
ST DEV	12.7605	0.4374	14.5615	5.1306	1.3857	1.5019	1.3475
SEM	7.3673	0.2525	8.4071	2.9622	0.8000	0.8671	0.7780

Table 3.6. Inhibition (%) as a function of exposure time, industrial ZnO, 10 mg/L.

concentration	50	mg/L					
Time (h)	0	5	12	24	48	72	96
Absorbance control 1	0.0130	0.0110	0.0120	0.0460	0.0720	0.0930	0.1020
Absorbance control 2	0.0170	0.0120	0.0130	0.0430	0.0680	0.0910	0.1050
Absorbance control 3	0.0140	0.0120	0.0150	0.0470	0.0690	0.0890	0.1070
Average absorbance of controls	0.0147	0.0117	0.0133	0.0453	0.0697	0.0910	0.1047
ST DEV	0.0021	0.0006	0.0015	0.0021	0.0021	0.0020	0.0025
SEM	0.0012	0.0003	0.0009	0.0012	0.0012	0.0012	0.0015
Absorbance sample 1	0.0120	0.0090	0.0140	0.0360	0.0390	0.0450	0.0480
Absorbance sample 2	0.0140	0.0110	0.0120	0.0350	0.0440	0.0460	0.0490
Absorbance sample 3	0.0150	0.0120	0.0110	0.0340	0.0410	0.0420	0.0510
Average absorbance of samples	0.0137	0.0107	0.0123	0.0350	0.0413	0.0443	0.0493
ST DEV	0.0015	0.0015	0.0015	0.0010	0.0025	0.0021	0.0015
SEM	0.0009	0.0009	0.0009	0.0006	0.0015	0.0012	0.0009
% inhibition	0.000	8.571	7.500	22.794	40.670	51.282	52.866
ST DEV	12.4748	9.1014	21.7224	4.5983	5.2696	1.7022	0.5022
SEM	7.2023	5.2547	12.5414	2.6549	3.0424	0.9828	0.2899

Table 3.7. Inhibition (%) as a function of exposure time, industrial ZnO, 50 mg/L.

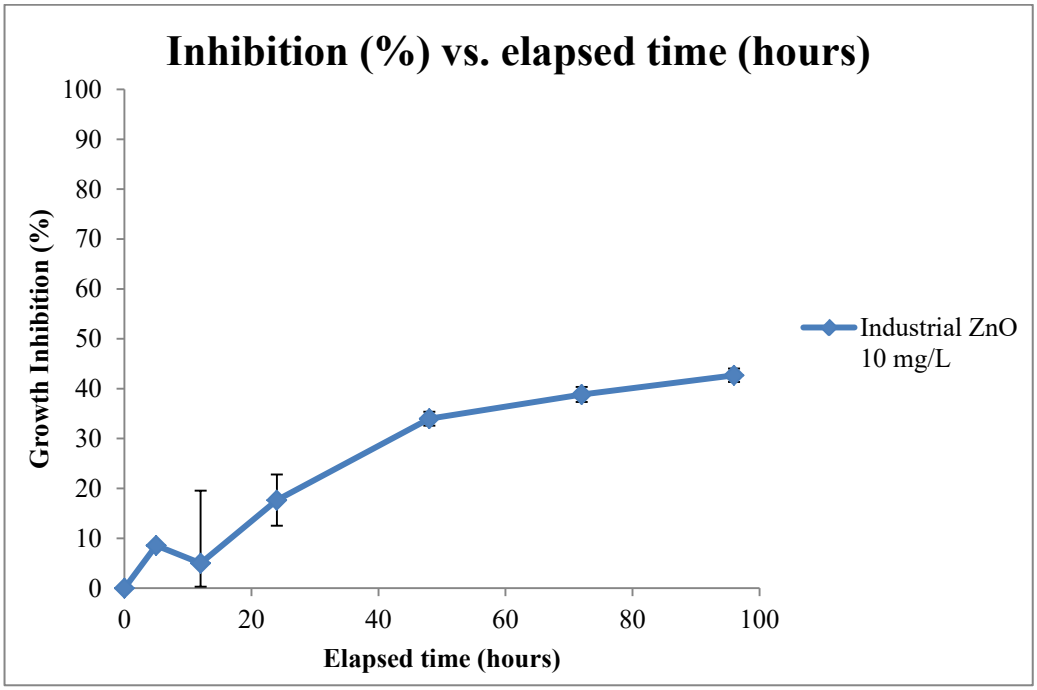

Figure 3.14. Inhibition (%) as a function of exposure time (0, 5, 12, 24, 48, 72, and 96 hrs) for 10 mg/L of industrial ZnO.

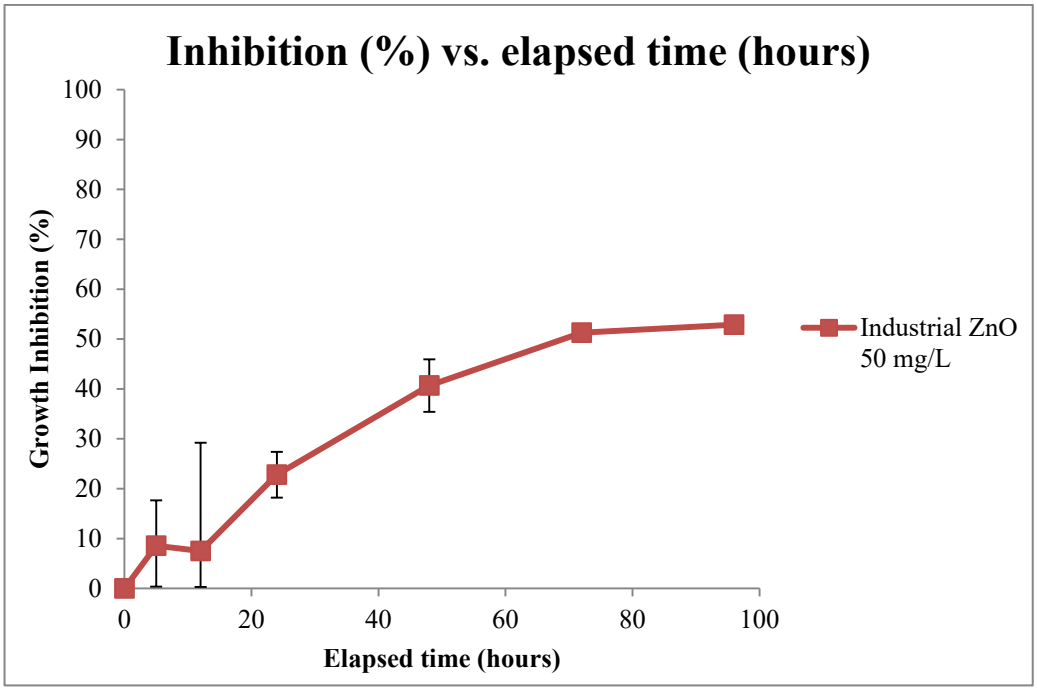

Figure 3.15. Inhibition (%) as a function of exposure time (0, 5, 12, 24, 48, 72, and 96 hrs) for 50 mg/L of industrial ZnO.

The purpose of this experiment was assessing the breakthrough time of nano-ZnO. As can be seen, both nanoparticles induce toxic effects toward the diatom cells. By looking at the experimental data plotted in Figure 3.14 and Figure 3.15, it can be noticed that measurements taken at a time lesser or equal to 24 hours have to be considered unreliable, due to physiological intrinsic variability of biological life: The triplicate experiments showed negligible growth inhibition. Indeed, the inhibition pattern observed from 0 to 24 hours post inoculation can be compared to the lag phase of the bacterial growth cycle portrayed in Figure 3.16[60]. During this phase, bacteria adapt to the environment and are unable to multiply.

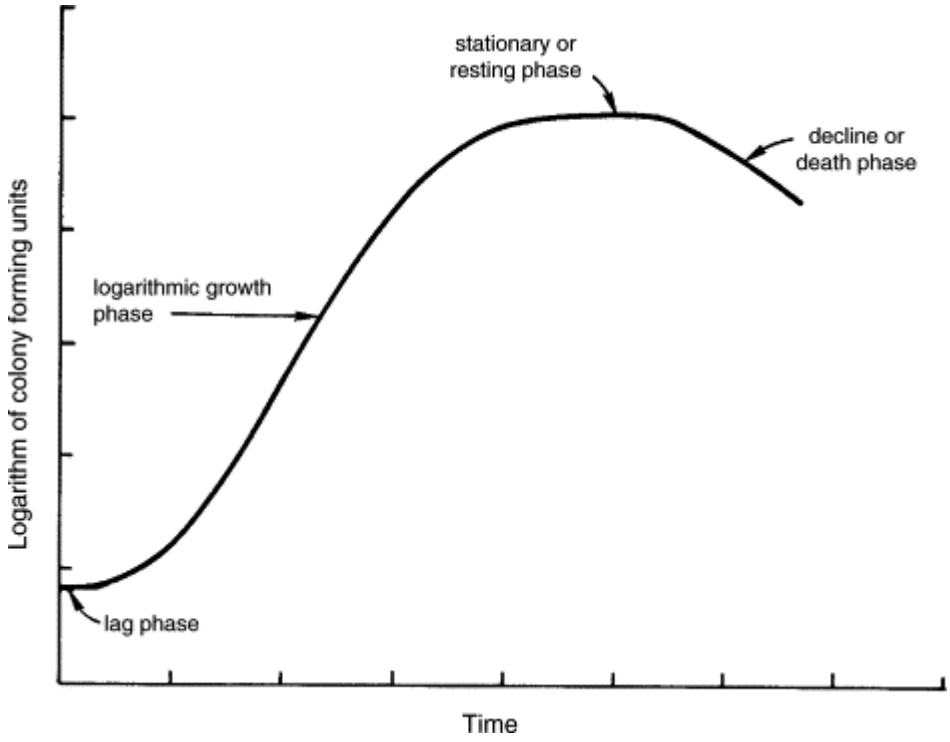

Figure 3.16. Typical bacterial growth curve.[60]

Therefore, data was estimated to be significant only from the subsequent measurement, i.e. 48 hours post inoculation. Moreover, since measurements taken at 48 hours present the first evidence of adverse toxic effect of nano-ZnO toward *Thalassiosira pseudonana* at both concentrations, this time was chosen as the breakthrough time for the next experiments.

3.6.4 Effect of ZnO concentrations at fixed exposure time

The results of the two experiments are presented in the following tables. In the first three rows of both tables it is possible to see the absorbance values, their average, and standard deviation for the three control samples. Then, it is possible to see the absorbance values, their average and standard deviation obtained for the three nano-ZnO samples (with concentrations of 1, 10, and 50 mg/L).

The inhibition (%) of *Thalassiosira pseudonana*, reported in column 4, was computed using the following formula, according to the study "Growth Inhibition and Induction of Apoptosis in SHG-44 Glioma Cells by Chinese Medicine Formula 'Pingliu Keli'" by Cao et al. (2011)[59]:

$$\%\ \text{inhibition (t)} = 100 - \ 100 * \frac{\text{average absorbance ZnO (t)}}{\text{average absorbance control (t)}}$$

Several statistical analysis were conducted:

- The standard deviation, σ, measuring the dispersion of a set of data, visible in rows 7, 13, and 16, is computed according to the following, where n = 3 and $\bar{x}$ is the average of the three samples:

$$\sigma = \sqrt{\frac{\sum(x-\bar{x})^2}{(n-1)}}$$

- The standard error of the mean, SEM, measuring the precision of the mean, visible in rows 8, 14, and 17, is computed according to the following:

$$SEM = \frac{\sigma}{\sqrt{n}}$$

- The Student's *t*-test (Two samples assuming equal variance), with the purpose of determining whether two data sets are significantly different from each other (control samples vs. nano-ZnO samples): Statistical significance ($p < 0.05$) was found for each data set.

The results of the first experiment are presented in Table 3.8 and Figure 3.17, while the results of the second experiment are presented in Table 3.9 and Figure 3.18.

Sample	Absorbance after 48h	Avg absorbance 48 h	% inhibition	ST. DEV.	SEM
Control 1	0.015	0.017	/	/	/
Control 2	0.017				
Control 3	0.018				
ZnO 1mg/l #1	0.012	0.012	28.00	3.4262	1.9781
ZnO 1mg/l #2	0.012				
ZnO 1mg/l #3	0.012				
ZnO 10mg/l #1	0.012	0.011	32.00	6.1647	3.5592
ZnO 10mg/l #2	0.012				
ZnO 10mg/l #3	0.010				
ZnO 50mg/l #1	0.009	0.009	44.00	1.7843	1.0302
ZnO 50mg/l #2	0.009				
ZnO 50mg/l #3	0.010				

Table 3.8. Inhibition (%) as a function of nano-ZnO concentration, first experiment.

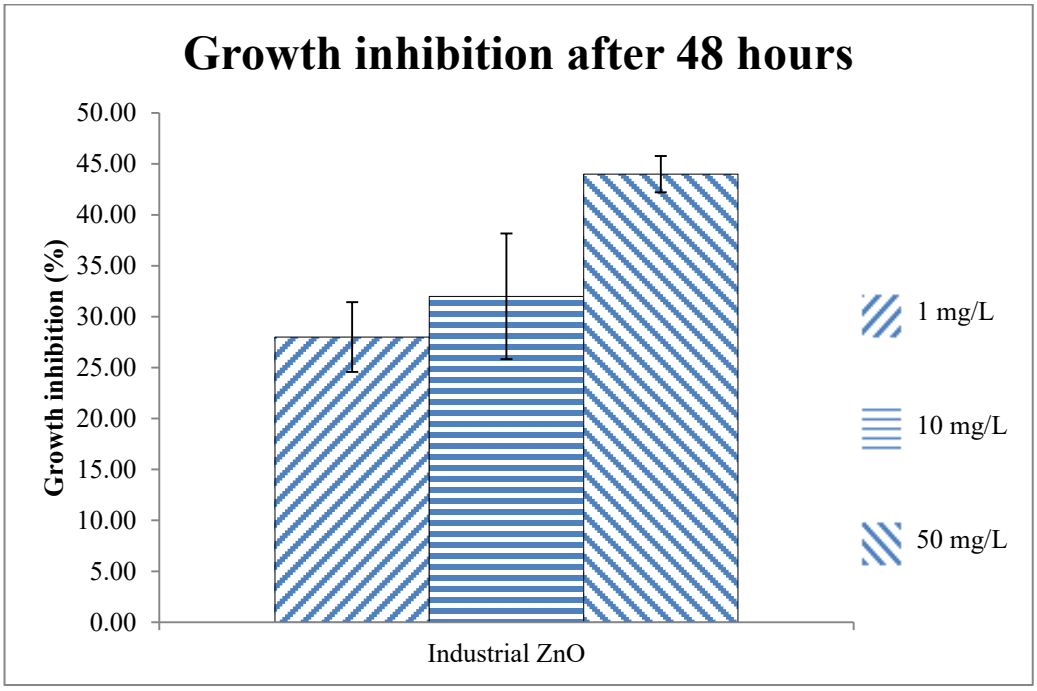

Figure 3.17. Inhibition (%) as a function of nano-ZnO concentration, first experiment.

Sample	Absorbance after 48h	Avg absorbance 48 h	% inhibition	ST. DEV.	SEM
Control 1	0.030	0.033	/	/	/
Control 2	0.028				
Control 3	0.041				
ZnO 1mg/l #1	0.033	0.029	13.13	9.6023	5.5439
ZnO 1mg/l #2	0.023				
ZnO 1mg/l #3	0.030				
ZnO 10mg/l #1	0.017	0.023	31.31	9.8842	5.7067
ZnO 10mg/l #2	0.026				
ZnO 10mg/l #3	0.025				
ZnO 50mg/l #1	0.016	0.020	40.40	9.0456	5.2225
ZnO 50mg/l #2	0.023				
ZnO 50mg/l #3	0.020				

Table 3.9. Inhibition (%) as a function of nano-ZnO concentration, second experiment.

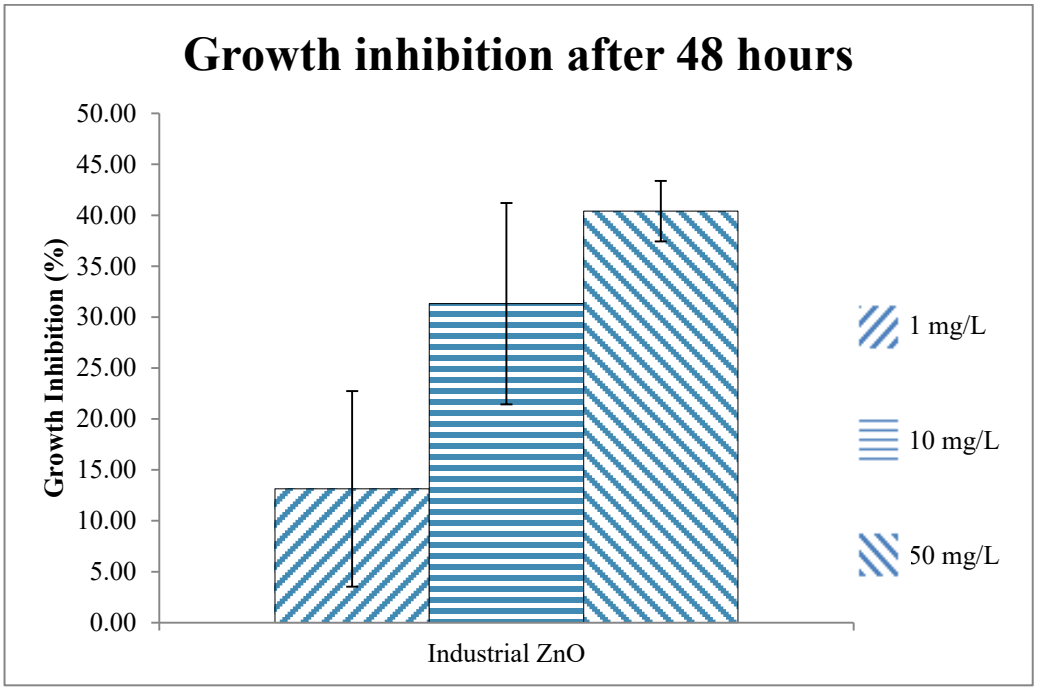

Figure 3.18. Inhibition (%) as a function of nano-ZnO concentration, second experiment.

Chapter 4 - Sunscreen nano-ZnO

The aim of the following experiments is testing the toxicity of sunscreen-derived zinc oxide nanoparticles to the diatom *Thalassiosira pseudonana*. The toxicity to the algal cells was expressed in terms of growth inhibition, which was estimated by the difference in the absorbance of the specimens with respect to the control sample. The experiments were performed at the Environmental Engineering Laboratory of the University of Miami.

4.1 Technical equipment

4.1.1 Beckman Coulter DU 720 Spectrophotometer

A Beckman Coulter DU 720 Spectrophotometer (Figure 3.1) is used in order to measure the absorbance (i.e., the amount of light absorbed by the sample); its specifications are listed in Chapter 3, section 4.1. Prior to running the experiment and measuring the absorbance of a sample, is it necessary to select an appropriate wavelength range and scan a blank sample.

4.1.2 Zetasizer Nano ZS90

A Zetasizer Nano ZS90 (Figure 3.2) is used to measure both the size of particles in an aqueous media and the zeta potential of the colloid; its specifications are listed in Chapter 3, section 4.2. Measurements can be taken by placing the aqueous media in the appropriate cuvette.

4.1.3 Verilux VT 10 - 5000 lux

A Verilux VT 10 - 5000 lux (Figure 3.4) is used in combination with an incubator in order to provide an optimal environment for the growth of Thalassiosira pseudonana. Its timer allows dark:light cycles, essential to the diatom due to its photosynthetic nature.

4.1.4 Orion™ pH meter and glass electrode

The pH meter Orion™ 720Aplus, visible in Figure 3.5, together with the glass electrode Orion™ 8156BNUWP, visible in Figure 3.6, was used on order to assess the solution's pH.

4.2 Manufacture of artificial seawater and f/2 medium

The diatom needs artificial seawater and f/2 medium in order to survive in the laboratory. Artificial seawater and f/2 medium were prepared in the laboratory according to Guillard et al. (1962)[51] and Keller et al. (1988)[52], using the protocol previously described in Chapter 3.

4.3 Nanoparticles

Sunscreen-derived ZnO nanoparticles were extracted from "Walgreens Clear Zinc" (5% ZnO, 4% Octocrylene) sunscreen[61], purchased from a local Walgreens store (Miami, FL). In order to extract nano-ZnO from sunscreen, the following experimental procedure was adopted, according to Barker & Branch (2008)[62] (modified version).

1. Weigh 3 g of sunscreen in a Falcon tube;
2. Add 30 mL of hexane (>99.9% purity, Honeywell Burdick & Jackson, Muskegon, MI) in the Falcon tube;
3. Sonicate for one minute, then centrifuge at 4400 revolutions per minute (rpm) for five minutes;
4. Discard the hexane solution and add 30 mL of ethanol (>95% purity, Pharmco-Aaper Shelbyville, KY)
5. Sonicate for one minute, then centrifuge at 4400 rpm for five minutes;
6. Discard the ethanol solution and add 30 mL of deionized (DI) water;
7. Shake the Falcon tube manually and centrifuge at 3000 rpm for 10 minutes;
8. Discard the solution on top of the Falcon tube and repeat step number 6 and 7 for two times;
9. Discard the solution on top of the Falcon tube and dry samples in oven at 100°C for at least 12 hours;
10. Place the samples in the desiccator.

A sterilized grinder is used to obtain a finer powder. The toxic effects of nano-ZnO were investigated by suspending 1, 10, and 50 mg of ZnO nanoparticles in 1 L of artificial seawater f/2 medium.

4.4 Diatom culture

Thalassiosira pseudonana cells were purchased from Bigelow Laboratory for Ocean Sciences (CCMP 1335)[54]. The culture of *Thalassiosira pseudonana* was obtained by adding artificial seawater f/2 medium to the originally purchased culture. Then the culture was incubated at a constant temperature of 26°C, with 12h:12h (dark:light) cycles maintained with Verilux VT 10 - 5000 lux.

4.5 Experimental setup

4.5.1 Detection of *Thalassiosira pseudonana* absorbance wavelength

In order to estimate the growth inhibition induced by sunscreen-derived nano-ZnO toward the marine diatom *Thalassiosira pseudonana*, several absorbance tests were performed. The aim of the experiment is to find a relationship between the absorbance measured with the spectrophotometer and the algae concentration in the samples. This indirect measurement of the growth inhibition was chosen due to the difficulties associated with direct measurements.

As already stated in Chapter 3, the issue associated with this type of indirect measurement was finding the wavelength corresponding to the algae's peak in the red band. A wide range of wavelengths were tested, and measurements assessed that the peak of absorption of *Thalassiosira pseudonana* occurred at a wavelength corresponding to 674 nm. The relationship between the absorbance of *Thalassiosira pseudonana* and its concentration in artificial seawater, for a wavelength of 674 nm can be seen in Figure 3.8. This value was used to analyze the changes in the absorbance of poisoned diatom cells in next experiments.

4.5.2 Inhibition (%) as a function of exposure time

For the triplicate experiment, 15 mL of nanoparticle suspension were inoculated in 15 mL of diatom culture and placed in a 50 mL Petri dish, gently mixing it afterwards. For sunscreen-derived nano-ZnO, two concentrations were tested: 10

and 50 mg/L. Control samples consisted in 15 mL of artificial seawater f/2 medium diluted into 15 mL of algae mass culture. The absorbance measurements were repeated at fixed time steps (0, 5, 12, 24, 48, 72, and 96 hours after inoculation).

4.5.3 Effect of ZnO concentrations at fixed exposure time

For the two triplicate experiments, 15 mL of nanoparticle suspension were inoculated in 15 mL of diatom culture and placed in a 50 mL Petri dish, gently mixing it afterwards. For sunscreen-derived nano-ZnO, three concentrations were tested: 1, 10 and 50 mg/L. Control samples consisted in 15 mL of artificial seawater f/2 medium into 15 mL of algae mass culture. Absorbance measurements were repeated after 48 hours.

4.6 Results

4.6.1 Zinc Oxide dissolution

The pH of *Thalassiosira pseudonana* exposed to sunscreen-derived nano-ZnO (50 mg/L), measured at 0 and 48 hours after inoculation, slightly increased from 8.5 to 8.6 (Spisni and Seo et al., 2016 submitted [58]).

4.6.2 Particle size

The particle size of sunscreen-derived zinc oxide nanoparticles, as mentioned in Spisni and Seo et al. (2016, submitted)[58] was assessed by means of X-Ray Diffraction (XRD) analysis. The measurement indicates that sunscreen-derived zinc oxide nanoparticles have a diameter equal to 31 nm.

A Zetasizer Nano ZS90 (Malvern Instrument, UK) was used in order to measure the particle size and the zeta potential of *Thalassiosira pseudonana* exposed to sunscreen-derived nano-ZnO (50 mg/L). The measurements, taken at 0 and 48 hours after inoculation, showed that the particle size increased from 1234 nm to 2217 nm, while the zeta potential decreased from -8.5 mV to -4.0 mV (Spisni and Seo et al., 2016 submitted[58]).

4.6.3 Inhibition (%) as a function of exposure time

The results of the experiments are presented in Table 4.1 and Table 4.2. In rows 3 to 7 it is possible to see the absorbance values, their average, and standard

deviation obtained for the three control samples. Then, in rows 9 to 13 it is possible to see the absorbance values, their average, and standard deviation obtained for the three ZnO samples (10 mg/L in Table 4.1 and 50 mg/L in Table 4.2).

The inhibition (%) of *Thalassiosira pseudonana*, reported in row 15, was computed using the following formula, according to the study "Growth Inhibition and Induction of Apoptosis in SHG-44 Glioma Cells by Chinese Medicine Formula 'Pingliu Keli'" by Cao et al. (2011)[59]:

$$\%\ \text{inhibition (t)} = 100 - 100 * \frac{\text{average absorbance ZnO (t)}}{\text{average absorbance control (t)}}$$

Several statistical analysis were conducted:

- The standard deviation, σ, measuring the dispersion of a set of data, visible in rows 7, 13, and 16, is computed according to the following, where n = 3 and $\bar{x}$ is the average of the three samples:

$$\sigma = \sqrt{\frac{\sum(x-\bar{x})^2}{(n-1)}}$$

- The standard error of the mean, SEM, measuring the precision of the mean, visible in rows 8, 14, and 17, is computed according to the following:

$$SEM = \frac{\sigma}{\sqrt{n}}$$

- The Student's *t*-test (Two samples assuming equal variance), with the purpose of determining whether two data sets are significantly different from each other (control samples vs. nano-ZnO samples): Statistical significance ($p < 0.05$) was found for each set of data with $t > 24$ hours.

The results of the experiments, reported in Table 4.1, and Table 4.2, are plotted in Figure 4.1, and Figure 4.2.

concentration	10	mg/L					
Time (h)	0	5	12	24	48	72	96
Absorbance control 1	0.0130	0.0110	0.0120	0.0460	0.0720	0.0930	0.1020
Absorbance control 2	0.0170	0.0120	0.0130	0.0430	0.0680	0.0910	0.1050
Absorbance control 3	0.0140	0.0120	0.0150	0.0470	0.0690	0.0890	0.1070
Average absorbance of controls	0.0147	0.0117	0.0133	0.0453	0.0697	0.0910	0.1047
ST DEV	0.0021	0.0006	0.0015	0.0021	0.0021	0.0020	0.0025
SEM	0.0012	0.0003	0.0009	0.0012	0.0012	0.0012	0.0015
Absorbance sample 1	0.0130	0.0120	0.0110	0.0410	0.0510	0.0580	0.0680
Absorbance sample 2	0.0160	0.0100	0.0130	0.0390	0.0480	0.0570	0.0690
Absorbance sample 3	0.0170	0.0110	0.0120	0.0380	0.0470	0.0580	0.0650
Average absorbance of samples	0.0153	0.0110	0.0120	0.0393	0.0487	0.0577	0.0673
ST DEV	0.0021	0.0010	0.0010	0.0015	0.0021	0.0006	0.0021
SEM	0.0012	0.0006	0.0006	0.0009	0.0012	0.0003	0.0012
% inhibition	0.000	5.714	10.000	13.235	30.144	36.630	35.669
ST DEV	14.3740	13.1434	10.0462	5.2909	1.5031	1.5458	3.1783
SEM	8.2988	7.5884	5.8002	3.0547	0.8678	0.8925	1.8350

Table 4.1. Inhibition (%) as a function of exposure time, sunscreen-derived ZnO, 10 mg/L.

concentration	50	mg/L					
Time (h)	0	5	12	24	48	72	96
Absorbance control 1	0.0130	0.0110	0.0120	0.0460	0.0720	0.0930	0.1020
Absorbance control 2	0.0170	0.0120	0.0130	0.0430	0.0680	0.0910	0.1050
Absorbance control 3	0.0140	0.0120	0.0150	0.0470	0.0690	0.0890	0.1070
Average absorbance of controls	0.0147	0.0117	0.0133	0.0453	0.0697	0.0910	0.1047
ST DEV	0.0021	0.0006	0.0015	0.0021	0.0021	0.0020	0.0025
SEM	0.0012	0.0003	0.0009	0.0012	0.0012	0.0012	0.0015
Absorbance sample 1	0.0160	0.0100	0.0130	0.0360	0.0450	0.0500	0.0570
Absorbance sample 2	0.0130	0.0110	0.0130	0.0390	0.0430	0.0470	0.0590
Absorbance sample 3	0.0140	0.0110	0.0120	0.0380	0.0440	0.0460	0.0570
Average absorbance of samples	0.0143	0.0107	0.0127	0.0377	0.0440	0.0477	0.0577
ST DEV	0.0015	0.0006	0.0006	0.0015	0.0010	0.0021	0.0012
SEM	0.0009	0.0003	0.0003	0.0009	0.0006	0.0012	0.0007
% inhibition	0.000	8.571	5.000	16.912	36.842	47.619	44.904
ST DEV	23.3035	0.4374	14.5615	6.5617	0.6367	1.2106	1.6040
SEM	13.4543	0.2525	8.4071	3.7884	0.3676	0.6989	0.9261

Table 4.2. Inhibition (%) as a function of exposure time, sunscreen-derived ZnO, 50 mg/L.

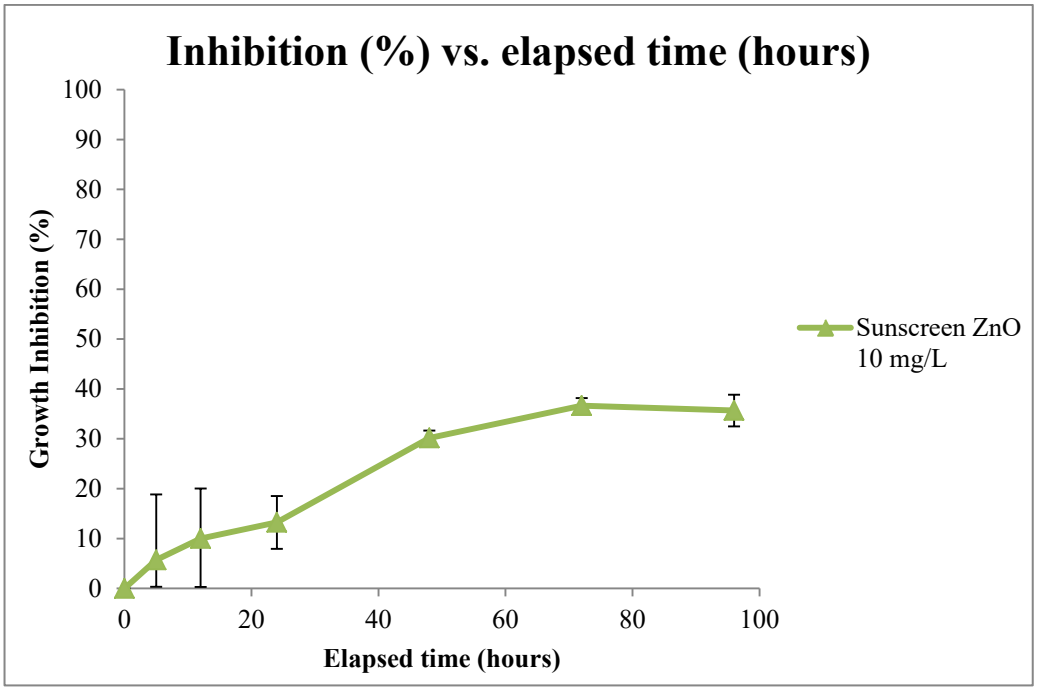

Figure 4.1.Inhibition (%) as a function of exposure time (0, 5, 12, 24, 48, 72, and 96 hrs) for 10 mg/L of sunscreen-derived ZnO.

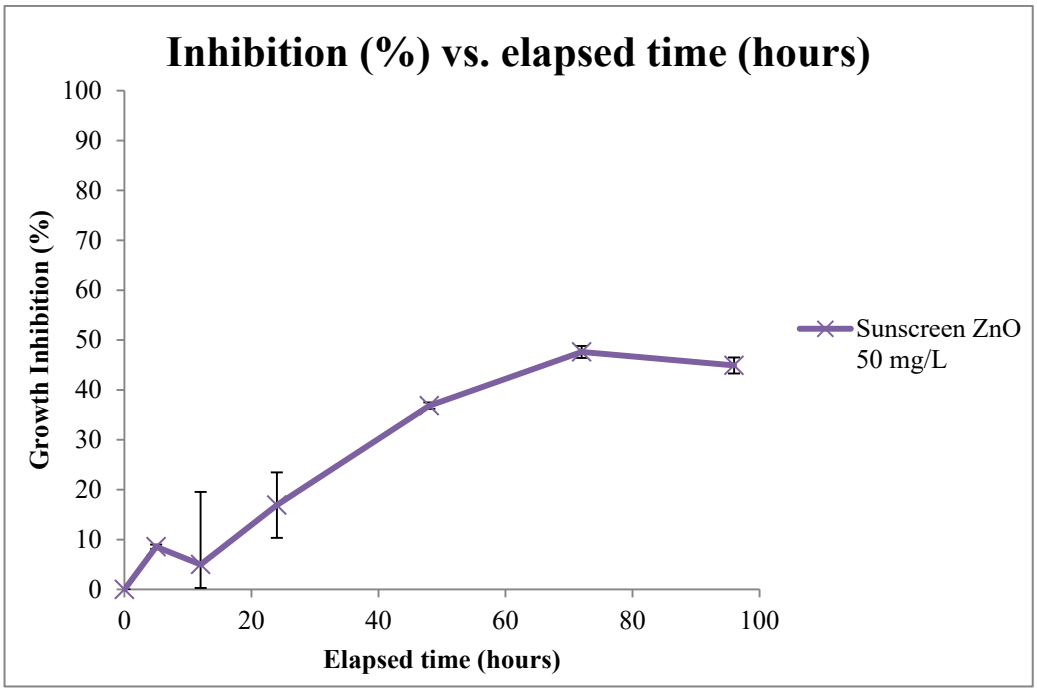

Figure 4.2. Inhibition (%) as a function of exposure time (0, 5, 12, 24, 48, 72, and 96 hrs) for 50 mg/L of sunscreen-derived ZnO.

The purpose of this experiment was assessing the breakthrough time of nano-ZnO. As can be seen, both nanoparticles induce toxic effects toward the diatom

cells. By looking at the experimental data plotted in Figure 4.1 and 4.2, it can be noticed that measurements taken at a time less or equal to 24 hours have to be considered unreliable, due to physiological intrinsic variability of biological life: The triplicate experiments showed negligible growth inhibition. Indeed, the inhibition pattern observed from 0 to 24 hours post inoculation can be compared to the lag phase of the bacterial growth cycle portrayed in Figure 3.14. During this phase, bacteria adapt to the environment and are unable to multiply. Therefore, data was estimated to be significant only from the subsequent measurement, i.e. 48 hours post inoculation. Moreover, since measurements taken at 48 hours present the first evidence of adverse toxic effect of nano-ZnO toward *Thalassiosira pseudonana* at both concentrations, this time was chosen as the breakthrough time for the next experiments.

4.6.4 Effect of ZnO concentrations at fixed exposure time

The results of the two experiments are presented in the Table 4.3 and Table 4.4. In the first three rows of both tables it is possible to see the absorbance values, their average, and standard deviation for the three control samples. Then, it is possible to see the absorbance values, their average and standard deviation obtained for the three nano-ZnO samples (with concentrations of 1, 10, and 50 mg/L).

The inhibition (%) of *Thalassiosira pseudonana*, reported in column 4, was computed using the following formula, according to the study "Growth Inhibition and Induction of Apoptosis in SHG-44 Glioma Cells by Chinese Medicine Formula 'Pingliu Keli'" by Cao et al. (2011)[59]:

$$\%\ \text{inhibition (t)} = 100 - \ 100 * \frac{\text{average absorbance ZnO (t)}}{\text{average absorbance control (t)}}$$

Several statistical analysis were conducted:

- The standard deviation, σ, measuring the dispersion of a set of data, visible in rows 7, 13, and 16, is computed according to the following, where n = 3 and $\bar{x}$ is the average of the three samples:

$$\sigma=\sqrt{\frac{\sum(x-\bar{x})^2}{(n-1)}}$$

- The standard error of the mean, SEM, measuring the precision of the mean, visible in rows 8, 14, and 17, is computed according to the following:

$$SEM=\frac{\sigma}{\sqrt{n}}$$

- The Student's *t*-test (Two samples assuming equal variance), with the purpose of determining whether two data sets are significantly different from each other (control samples vs. nano-ZnO samples): Statistical significance ($p < 0.05$) was found for each set of data.

The results of the first experiment are presented in Table 4.3 and Figure 4.3, while the results of the second experiment are presented in Table 4.4 and Figure 4.4.

Sample	Absorbance after 48h	Avg absorbance 48 h	% inhibition	ST. DEV.	SEM
Control 1	0.015	0.017	/	/	/
Control 2	0.017				
Control 3	0.018				
ZnO 1mg/l #1	0.013	0.014	14.00	1.2517	0.7227
ZnO 1mg/l #2	0.015				
ZnO 1mg/l #3	0.015				
ZnO 10mg/l #1	0.012	0.012	30.00	6.6063	3.8141
ZnO 10mg/l #2	0.013				
ZnO 10mg/l #3	0.010				
ZnO 50mg/l #1	0.007	0.011	36.00	9.2111	5.3180
ZnO 50mg/l #2	0.005				
ZnO 50mg/l #3	0.007				

Table 4.3. Inhibition (%) as a function of nano-ZnO concentration, first experiment.

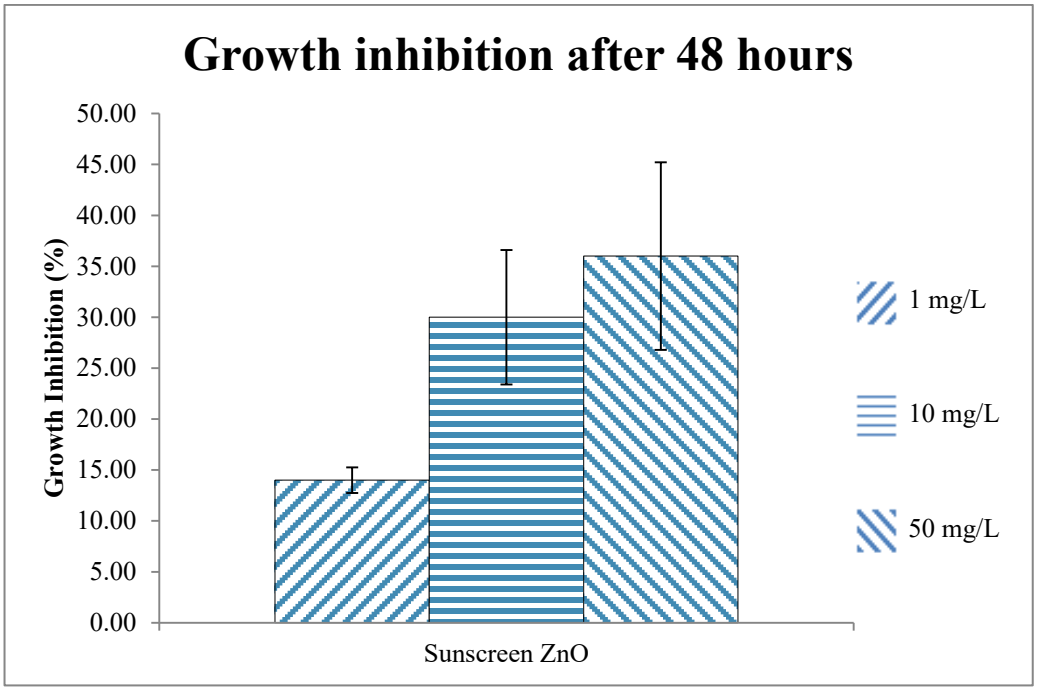

Figure 4.3. Inhibition (%) as a function of nano-ZnO concentration, first experiment.

Sample	Absorbance after 48h	Avg absorbance 48 h	% inhibition	ST. DEV.	SEM
Control 1	0.030	0.033	/	/	/
Control 2	0.028				
Control 3	0.041				
ZnO 1mg/l #1	0.035	0.030	8.08	12.2868	7.0938
ZnO 1mg/l #2	0.028				
ZnO 1mg/l #3	0.028				
ZnO 10mg/l #1	0.027	0.025	24.24	8.5317	4.9258
ZnO 10mg/l #2	0.024				
ZnO 10mg/l #3	0.024				
ZnO 50mg/l #1	0.019	0.020	38.38	2.9658	1.7123
ZnO 50mg/l #2	0.019				
ZnO 50mg/l #3	0.023				

Table 4.4. Inhibition (%) as a function of nano-ZnO concentration, second experiment.

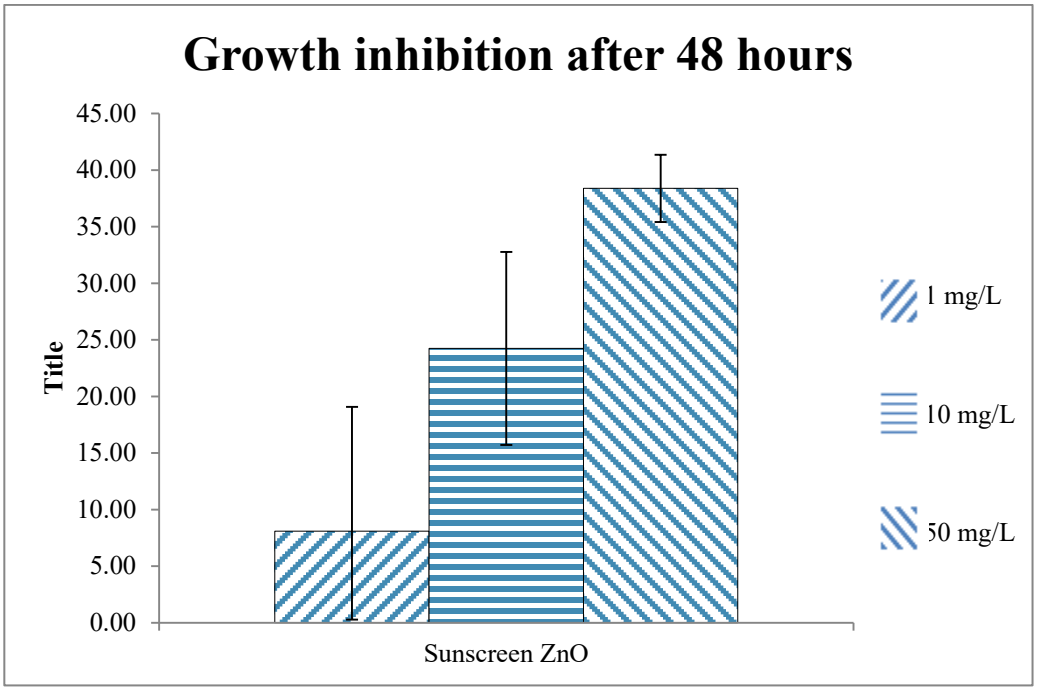

Figure 4.4. Inhibition (%) as a function of nano-ZnO concentration, second experiment.

Chapter 5 - Comparison of results and discussion

The results of the two experiments were then grouped in order to analyze them; the first three comparisons (Fig.5.1 to Fig.5.4) are based on the first experiment (i.e., inhibition as a function of exposure time), whereas the fourth comparison (Fig.5.5) is based on the second experiment (i.e., ZnO concentrations at fixed exposure time).

The first comparison regards the growth inhibition (%) induced by either industrial and sunscreen nano-ZnO nanoparticles as a function of the elapsed time. The nanoparticles have concentrations equal to 10 and 50 mg/L. As can be seen in Figure 5.1 and Figure 5.2, the growth inhibition *of Thalassiosira pseudonana* appears to be influenced by the exposure time to the nanoparticles, for fixed pollutant concentration. On the other hand, it is possible to notice that the growth inhibition, induced by both concentrations, has a similar trend; therefore it is possible to hypothesize that the nano-ZnO concentration plays a smaller, but measurable, role in the toxicity toward the diatom.

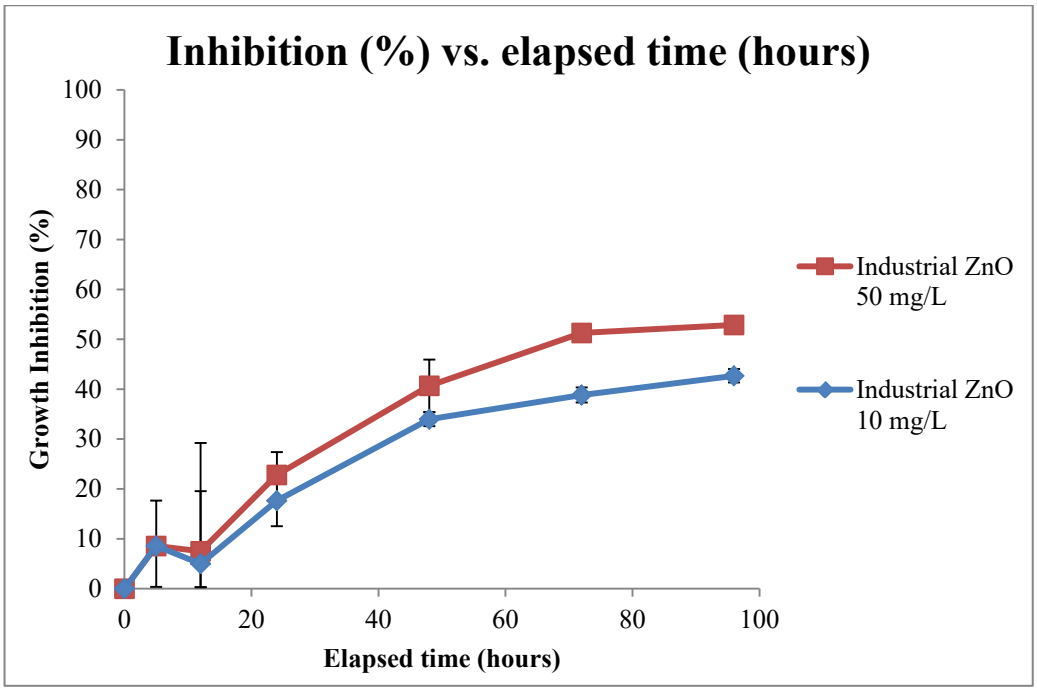

Figure 5.1. Inhibition (%) as a function of exposure time, 10 and 50 mg/L, industrial nanoparticles.

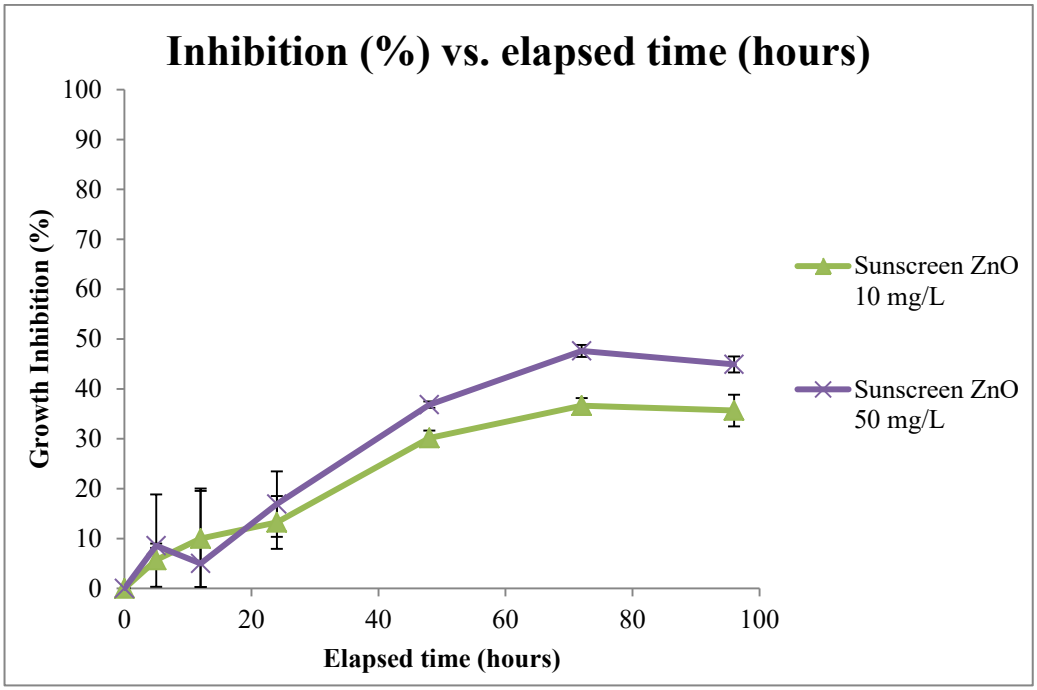

Figure 5.2. Inhibition (%) as a function of exposure time, 10 and 50 mg/L, sunscreen-derived nanoparticles.

The second comparison regards the growth inhibition (%) induced by industrial- and sunscreen-derived ZnO nanoparticles. Figure 5.3 plots the results of the experiments performed with diatoms exposed to 10 mg/L of industrial- and sunscreen-derived nano-ZnO in the aqueous media; Figure 5.4 plots the results of the experiments performed with diatoms exposed to 50 mg/L of industrial- and sunscreen-derived nano-ZnO in the aqueous media. As can be seen from both Figure 5.3 and Figure 5.4, industrial-derived zinc oxide nanoparticles appear to be inducing slightly greater toxic effects toward *Thalassiosira pseudonana*, when compared to sunscreen-derived zinc oxide nanoparticles. Moreover, the difference in the growth inhibition appears to be increasing with the exposure time.

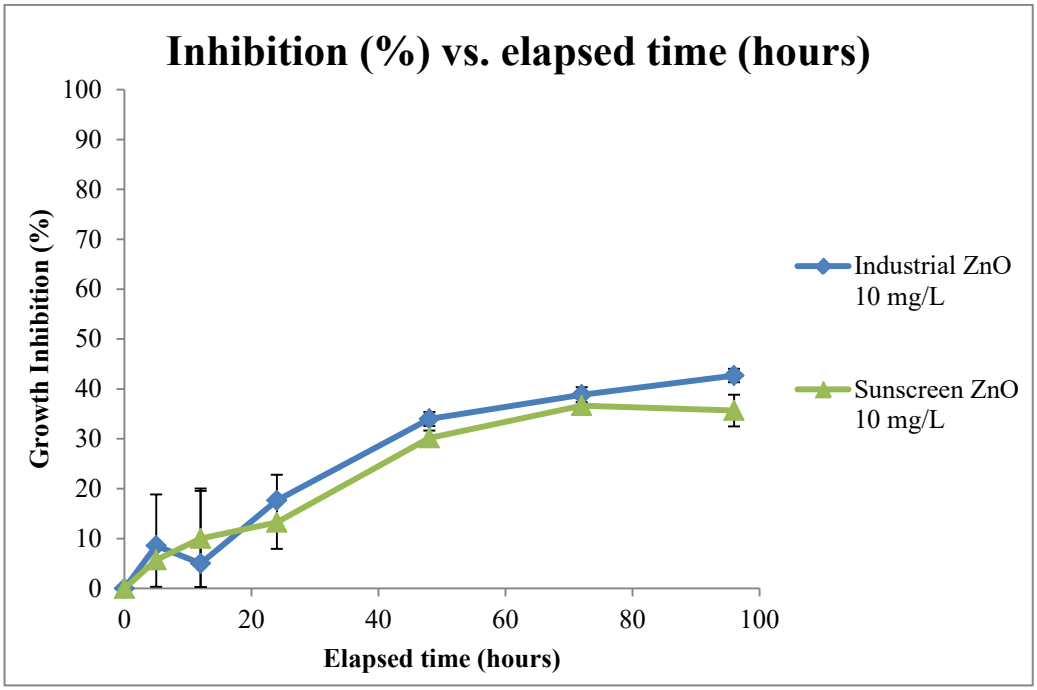

Figure 5.3. Inhibition (%) as a function of exposure time, comparison of industrial and sunscreen, 10 mg/L.

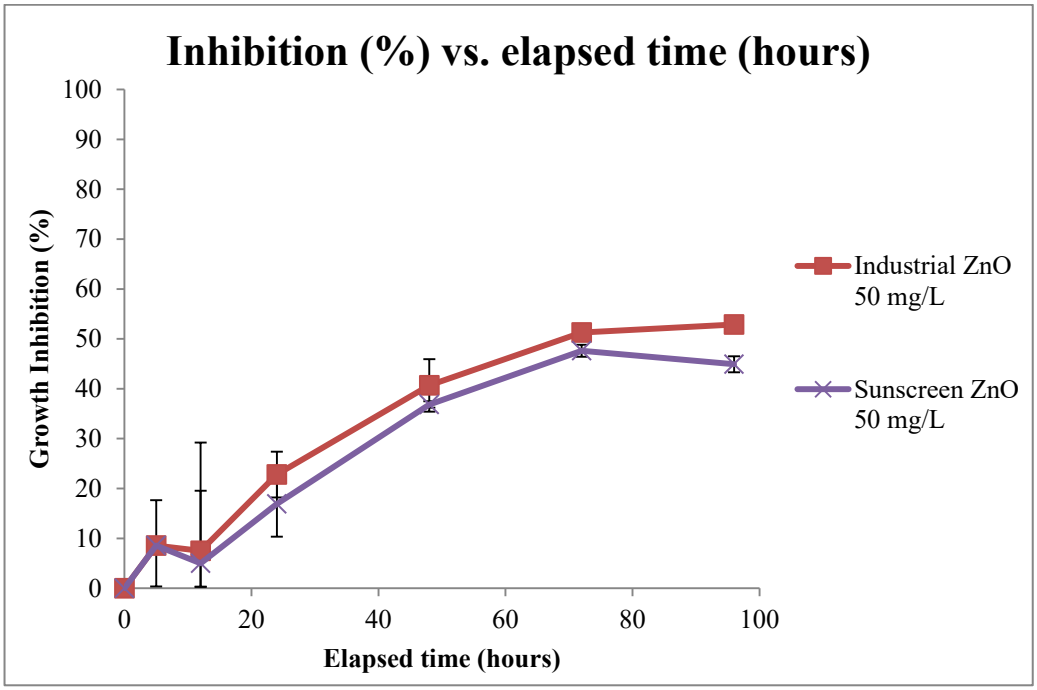

Figure 5.4. Inhibition (%) as a function of exposure time, comparison of industrial and sunscreen, 50 mg/L.

The third comparison regards the growth inhibition induced by industrial- and sunscreen-derived ZnO nanoparticles, as a function of the elapsed time. Figure 5.5 plots the results of the experiments performed with diatoms exposed to both 10 and 50 mg/L of industrial- and sunscreen-derived nano-ZnO in the aqueous media. This plot accentuates the outcomes already mentioned analyzing Fig. 5.1 to Fig. 5.4. Indeed, it is possible to see that the growth inhibition of *Thalassiosira pseudonana*:

- May depend on the type of ZnO nanoparticle (industrial- or sunscreen-derived) dispersed in the aqueous media, when exposed to constant nano-ZnO concentrations;
- May depend on the exposure time to the ZnO nanoparticles dispersed in the aqueous media; and
- Is slightly influenced by the concentration of the ZnO nanoparticles dispersed in the aqueous media.

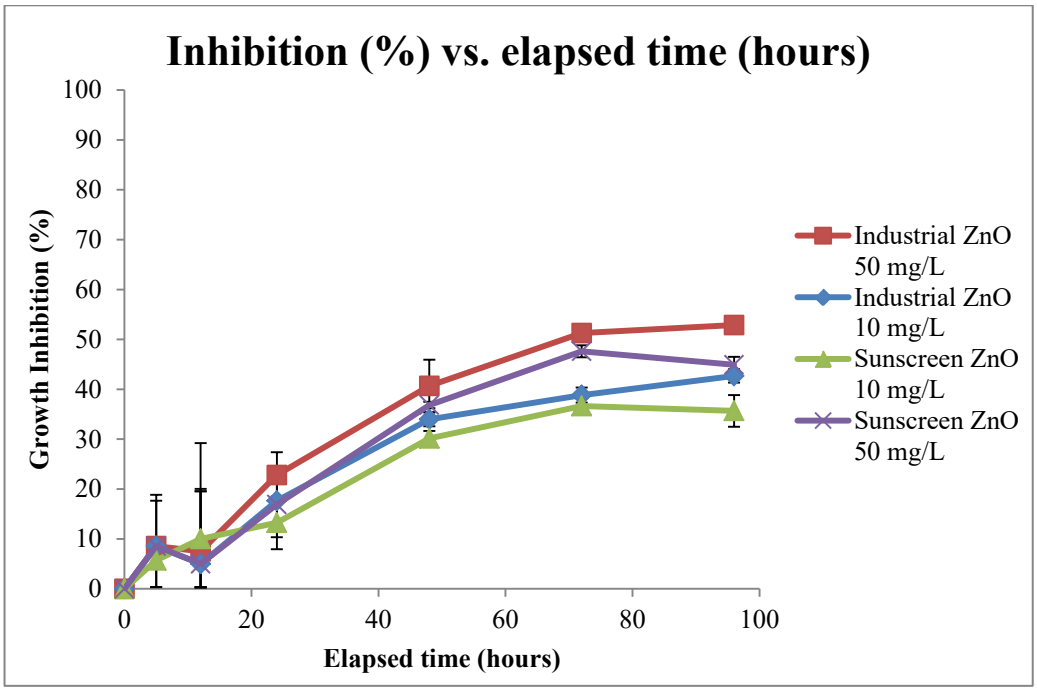

Figure 5.5. Inhibition (%) as a function of exposure time.

The overall results of the second set of experiments, regarding the growth inhibition (%) as a function of the nanoparticle concentration at 48 hours post inoculation, can be seen in Figure 5.6. The results show that the growth inhibition of

Thalassiosira pseudonana is associated with the concentration of zinc oxide nanoparticles in the aqueous media: Indeed the experiments show that, after 48 hours of incubation, an incremental increase of the concentration of nanosized metal oxide nanoparticles corresponded to greater growth inhibition of the diatom.

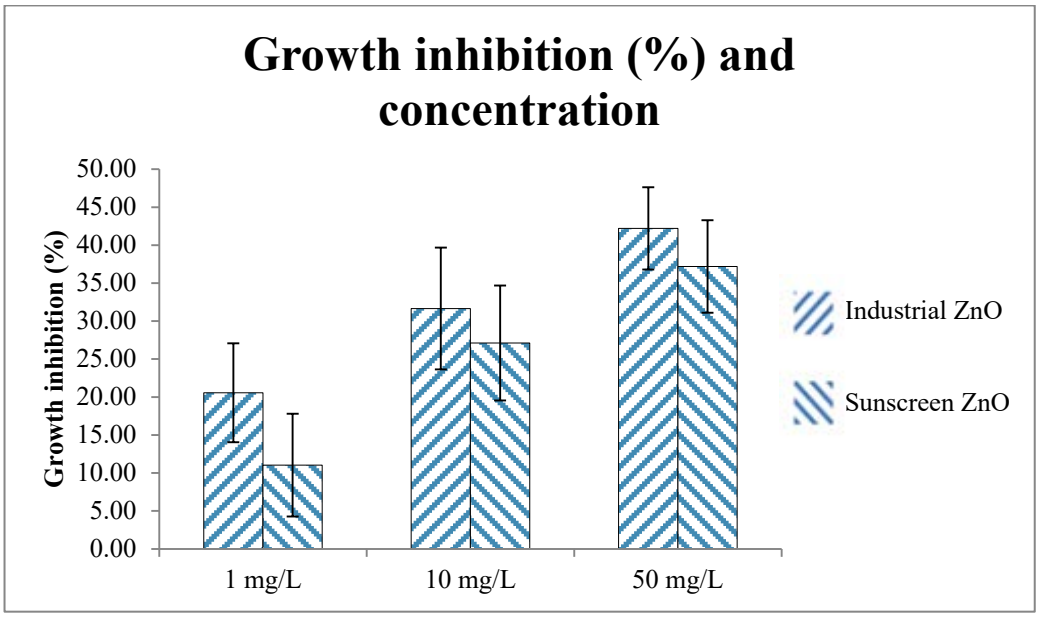

Figure 5.6. Inhibition (%) as a function of nano-ZnO concentration, 48 hours post inoculation.

Moreover, it is possible to notice that industrial-derived nano-ZnO seems to be inducing greater toxic effects toward *Thalassiosira pseudonana* compared to sunscreen-derived nano-ZnO, at each nanoparticle concentration (i.e., 1 mg/L, 10 mg/L, and 50 mg/L).

In addition, it should be noticed that the highest discrepancy in the growth inhibition induced by industrial- and sunscreen-derived nano-ZnO was found at the lowest nanoparticle concentration (i.e., 1 mg/L): The growth inhibition induced by industrial-derived nano-ZnO was found two times greater than the growth inhibition induced by sunscreen-derived nano-ZnO; on the other hand higher nanoparticle concentrations (i.e., 10 mg/L and 50 mg/L) accounted for lower and similar discrepancies.

Summarizing the outcomes of the experiments, it is possible to see that the growth inhibition (effect of ZnO concentrations at fixed exposure time) of *Thalassiosira pseudonana*:

- May depend on the type of ZnO nanoparticle (industrial- or sunscreen-derived) dispersed in the aqueous media; and
- May depend on the concentration of the ZnO nanoparticles dispersed in the aqueous media.

Chapter 6 - Literature survey

The results of the growth inhibition experiments, performed on *Thalassiosira pseudonana* exposed to industrial-derived and sunscreen-derived zinc oxide nanoparticles, were then compared to the available bibliography, with the purpose of attempting to estimate the factors that could have led to the aforementioned outcomes. The study "Toxicity of Ag, CuO and ZnO nanoparticles to selected environmentally relevant test organisms and mammalian cells in vitro: a critical review" by Bondarenko et al. (2013)[63] establishes that, based on the existing literature, algae are the organisms suffering the greatest toxic effects induced by zinc oxide nanoparticles. Indeed, the study reports a median lethal (or effect) dose for half of the initial population of algal cells ($L(E)C_{50}$) of 0.08 mg/L; this concentration, compared to other organisms' nano-ZnO $L(E)C_{50}$, is the lowest one and, therefore, this metal oxide has been classified as "Very Toxic" for the algae group. Moreover, the review "The Toxic Effects and Mechanisms of CuO and ZnO Nanoparticles" by Chang et al. (2012)[64] reports that, for aquatic organisms, zinc oxide nanoparticles appear to be more toxic compared to its bulk version, due to the difference in size and to the transformation of its physical and chemical properties. The difference in toxicity induced by these two versions of the same nanoparticles will be further interrogated in the following paragraphs.

Additionally, it should be borne in mind that the factors taken into account and listed below are reasonably not independent of one another and their interaction is not merely plausible: Due to the complex chemical biological mechanisms involved in the processes, their coaction is reasonably inevitable and, therefore, there will be connections and cross-references throughout the survey.

6.1 Concentration effect

Many studies observed a remarkable correlation between the nano-ZnO concentration in the aqueous media and the toxicity (i.e., growth inhibition) toward algal cells. In particular, as can be guessed, many researches indicate a remarkable proportionality in the toxicity toward the tested organisms to the degree of concentration of the nanoparticles in solution. In particular, a greater growth inhibition was found for diatoms as a consequence of the increment of pollutant

concentration in the aqueous media. The same effects were observed during the experiments performed in the Environmental Engineering Laboratory of the University of Miami, while testing the toxicity of both industrial-derived and sunscreen-derived nano-ZnO toward *Thalassiosira pseudonana* in artificial seawater: The diatom was revealed to be subjected to greater growth inhibition when exposed to a greater concentration of nanoparticles. This effect was particularly visible during the second experiment (i.e. effect of ZnO concentrations at fixed exposure time), where three different concentrations of industrial- and sunscreen-derived zinc oxide nanoparticles (i.e. 1 mg/L, 10 mg/L, and 50 mg/L) were used to test the growth inhibition of *Thalassiosira pseudonana* 48 hours post inoculation. On the other hand, other studies point out that the mere concentration might be meaningless when investigating the toxicity, if the particle size is not taken into account. The review "Nanomaterials and nanoparticles: Sources and toxicity" by Buzea et al. (2007)[65] remarks that, considering two equal mass doses of pollutant, the one with smaller nanoparticles might be more toxic than the one with larger nanoparticles, due to the different amount of polluting surface area. An in-depth analysis of the degree of involvement of the particle size and surface area in the toxicity toward diatoms will be provided in the relative sections.

6.2 Particle size and particle shape effect

One of the factors that could have played a key role in contributing to the toxicity of nano-ZnO toward *Thalassiosira pseudonana* is the particle size. As already mentioned in Section 3.6.2, concerning the industrial-derived nanoparticles used for the growth inhibition test performed in the laboratory, measurements showed a particle size of 24 nm; on the other hand, as already mentioned in Section 4.6.2, concerning the sunscreen-derived nanoparticles used for the growth inhibition test performed in the laboratory, measurements showed a particle size of 31 nm. Besides, the particle size of *Thalassiosira pseudonana*, exposed to 50 mg/L of industrial-derived and sunscreen-derived nano-ZnO (0 and 48 hours after inoculation), can be seen in Table 6.1 (Spisni and Seo et al., 2016 submitted)[58].

	Particle size (nm)	
	0 hours	48 hours
Industrial nano-ZnO, 50 mg/L	1549	1574
Sunscreen nano-ZnO, 50 mg/L	1234	2217

Table 6.1. Particle size of polluted samples, 0 and 48 hours after inoculation[58].

The study "Cytotoxicity of ZnO NPs toward fresh water algae Scenedesmus obliquus at low exposure concentrations in UV-C, visible and dark conditions" by Bhuvaneshwari et al. (2015)[66] investigated the role of particle size in the inhibition of algal cells. After performing several experiments, it was established that the smaller particles, the greater the toxicity. The results of the experiments are presented in Figure 6.1, where ZnO-1 is the zinc oxide nanoparticle having a larger diameter, whereas ZnO-2 is the particle with a smaller diameter. The tests indicate that the presence of small particles have influenced three other factors that are widely known for being directly connected to cytotoxicity, listed as follows:

- Ionic release of Zn^{+2};
- ROS production; and
- Membrane integrity.

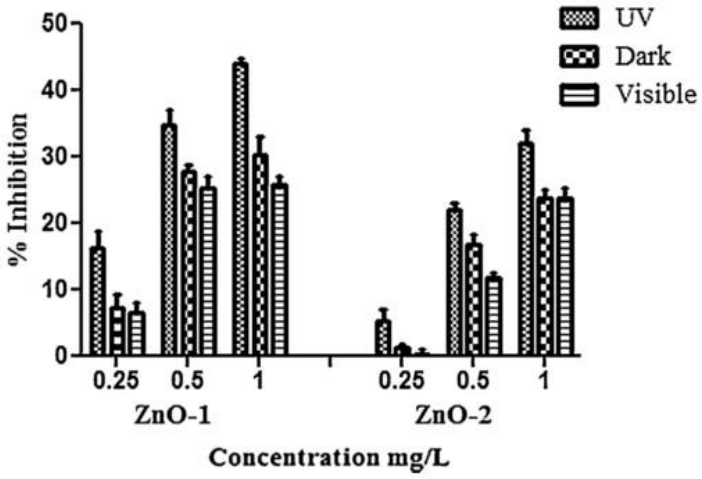

Figure 6.1. Growth inhibition vs. nanoparticle concentration, for different particle size[66].

Furthermore, other studies[67,68] indicate that metal oxide nanoparticles are more cytotoxic compared to their bulk version, and that the toxic effects become more and more evident as particle size decreases.

Moreover, many studies[16,17,65,69] reported that particle shape might be responsible for inducing toxic effects toward various organisms. In particular, nanoparticles with an elongated shape are more likely to pierce the cellular membrane and penetrate onto the cells. As reported in the study "Release and Toxicity comparison between industrial- and sunscreen-derived nanoZnO particles" by Spisni and Seo et al. (2016, submitted)[58], Scanning Electron Microscopy (SEM) images revealed that the nanoparticles used in the present case study were characterized by a spherical shape. Therefore, particle shape might be playing a non-significant role in the toxic effects observed during the aforementioned experiments.

Comparing the available bibliography to the present case study, it can be noticed that industrial-derived nanoparticles have smaller dimensions compared to the sunscreen-derived ones. Therefore, it seems reasonable to ascribe at least part of the toxic effects toward the diatom to the particle size. However, the difference in size between the two types of nanoparticles used for the growth rate inhibition experiments presented in the previous chapters is not excessively broad: 24 nm is the size of industrial-derived particles and 31 nm is the size of sunscreen-derived ones. Since the two nanoparticles account for a variation of only 7 nm, it seems appropriate to affirm that particle size cannot be accounted as the only factor influencing the toxicity toward *Thalassiosira pseudonana* in the present case study. Indeed, since aggregation is likely to happen at higher nano-ZnO concentrations, particle size might be listed among the factors influencing the diatom's growth inhibition at lower concentrations (i.e. 1 mg/L).

6.3 Ionic dissolution effect

The dissolution of ZnO into Zn^{2+} ions in the aqueous media, and the consequent uptake by algal cells, is one of the most investigated factors concerning the toxicity of this nanoparticle. As mentioned in the study "Effect of pH and impurities on the surface charge of zinc oxide" by Degen et al. (1999)[70], the reactions in aqueous solution that lead to the release of Zn^{2+} in water with pH of 7.5 are listed as follows:

$$ZnO\ (s) + H_2O\ (l) \leftrightarrow Zn(OH)_2\ (s)$$

$$Zn(OH)_2\ (s) \leftrightarrow Zn(OH)^+\ (aq) + OH^-\ (aq)$$

$$Zn(OH)^+\ (aq) \leftrightarrow Zn^{2+}\ (aq) + OH^-\ (aq)$$

While the net overall reaction can be expressed in the following terms:

$$ZnO\ (s) \leftrightarrow Zn^{2+}\ (aq) + OH^-\ (aq)$$

These reactions show how the ionization can take place, starting from a zinc oxide molecule into the aqueous media and ending with the generation of Zn^{2+} ions.

Regarding toxicity, Bhuvaneshwari et al. (2015)[66] have linked the amount of ions released in the suspension to the initial concentration of nano-ZnO, to the exposure time and, finally, to the particle size. In particular, it was discovered that:

- The ionic release is greater for high initial concentrations of polluting nanoparticles;
- The ionic release is maximum at an exposure time equal to 48 hours (i.e. the equilibrium concentration is reached after 48 hours); and
- The ionic release decreases with larger particle size.

These three effects are presented in Figure 6.2a and 6.2b.

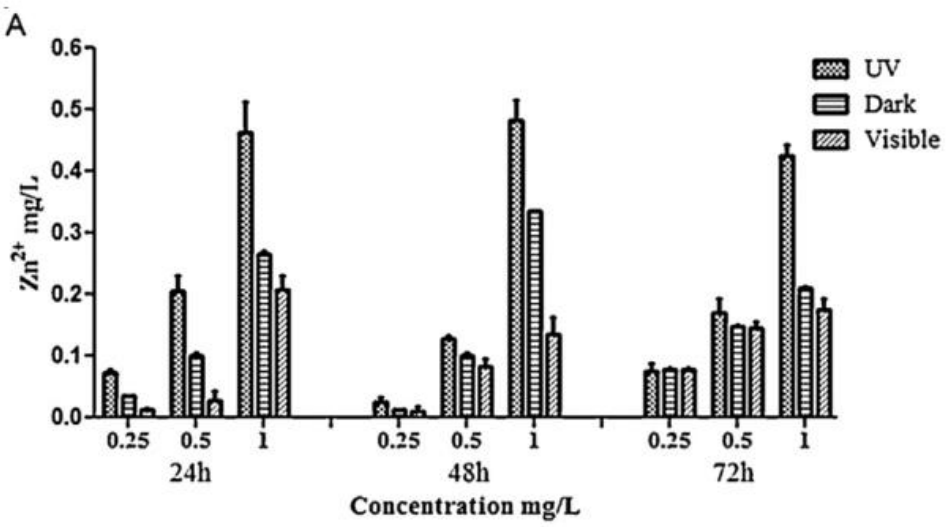

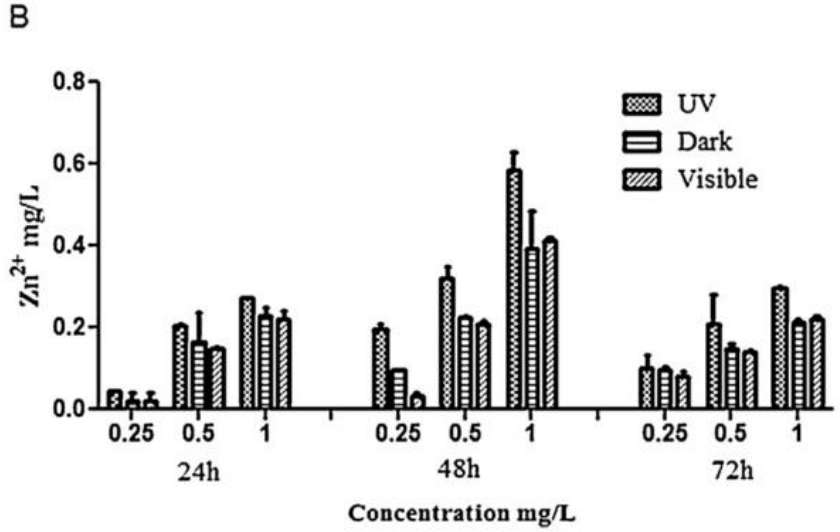

Figure 6.2. Ionic release as a function of time and nanoparticle concentration. A) ZnO-1 (smaller particles); B) of ZnO-2 (larger particles)[66].

In addition to the previously mentioned results, the experiments showed that the aqueous solutions containing a higher concentration of Zn^{2+} ions induced greater toxicity to the inoculated algae, compared to those solutions containing a lower amount of the aforementioned ions.

The review by Chang et al. (2012)[64] mentions that metal oxide nanoparticles, being much smaller and having a greater surface area than their bulk version, can release ions in a faster way, leading to greater toxic effects.

The study "Impacts of metal oxide nanoparticles on marine phytoplankton" by Miller et al. (2010)[71] indicates that the ionic dissolution, aggregation and sedimentation of nano-ZnO in natural seawater are processes that occur rapidly. A closer look at their results reveals that while ionic dissolution is faster at low particle concentration, aggregation and sedimentation are more rapid at higher particle concentration. The subsequent toxicity tests revealed that *Thalassiosira pseudonana* experienced a growth inhibition up to three times higher for a nanoparticle concentration of 1000 μg/L, compared to the control sample (0 μg/L) , as presented below in Figure 6.3.

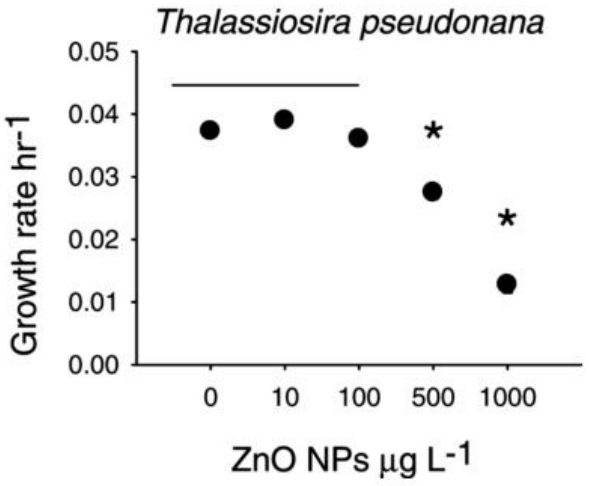

Figure 6.3. Growth rate of *Thalassiosira pseudonana* vs. ZnO nanoparticle concentration[71].

The study "Zinc oxide-engineered nanoparticles: Dissolution and toxicity to marine phytoplankton" by Miao et al. (2010)[72] concluded that the overall toxic effects of nano-ZnO toward *Thalassiosira pseudonana* could be justified by the mere presence of Zn^{2+} ions released by the nanoparticles in the aqueous media and not by the presence of the nanoparticles themselves; moreover, the release of ions was assessed to be greater in artificial seawater rather than in deionized water, while the concentration did not sufficiently influenced the reaction.

In the present case study, experiments showed a constant pH of 8.5; this pH, according to Figure 3.12 and Figure 3.13, suggests that ionic dissolution is not likely to affect the toxicity of the nanoparticles toward the diatom *Thalassiosira pseudonana*.

6.4 Aggregation, isoelectric point, and zeta potential effect

A colloid[73] is a disperse system in which two phases are simultaneously present: The first phase is acting as a medium (continuous phase), while the second phase is an insoluble substance made of small particles (dispersed phase). The continuous phase can be either in gas, solid or liquid form. Specifically, in this case study the particles suspended have dimensions between 1 and 1,000 nm, and the continuous phase is made of artificial seawater.

The Tindall effect is a very useful method to distinguish a solution and a colloid. In a solution, due to the very small diameter of the particles, the light path is

invisible. For colloids (in which the particles are insoluble and so their dimensions are greater and compatible to the wavelength of the light) the path is clearly visible and the light is scattered (Fig.6.4).

In colloidal chemistry what is important is the boundary zone between the two phases, i.e., their interface. The aquatic molecules symmetrically surround the nanoparticle and this creates interfacial tension.

Figure 6.4. Tyndall effect: In the solution (right glass) the light path is invisible, while for the colloid (left glass) the light path is visible[74].

For nanoparticles like zinc oxide, OH^- anion adsorbs to the particle interface and negatively charge the particle; this negative particle attracts positive particles, generating a difference in its potential. This Double Layer (DB), consisting of a first layer of positive ions and a second layer of positive and negative ions, contributes to the definition of the zeta potential (Fig.6.5), which can be used as an indicator of the stability of a colloid, since it expresses the degree of repulsion between the particles dispersed in the media. Therefore, the higher the zeta potential, the more stable the colloid. When the zeta potential is lower, the energy barrier resulting from the repulsion of the identically charged particles, becomes weaker and the particle aggregation starts.

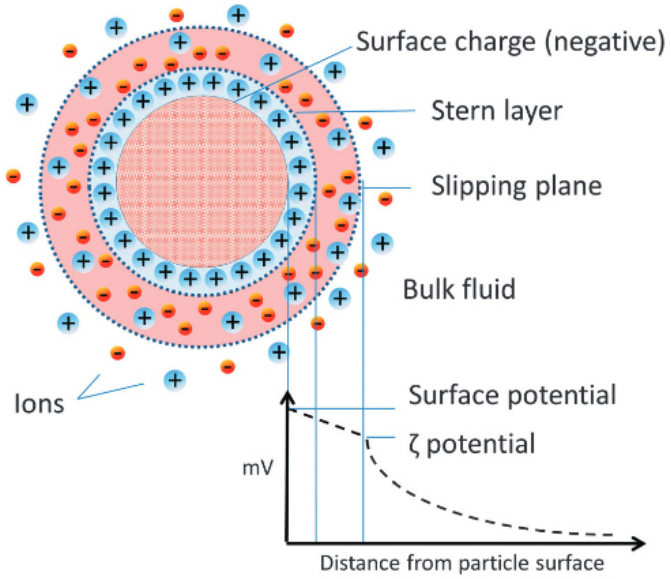

Figure 6.5. Zeta potential in colloids[75].

The DLVO theory, an acronym named after the four scientists who unveiled it (Boris Derjaguin, Lev Landau, Evert Verwey and Theodoor Overbeek), is used to explain the behavior and the stability of colloids, relating Van der Waals attraction and electrostatic repulsion, as can be seen in Figure 6.6.

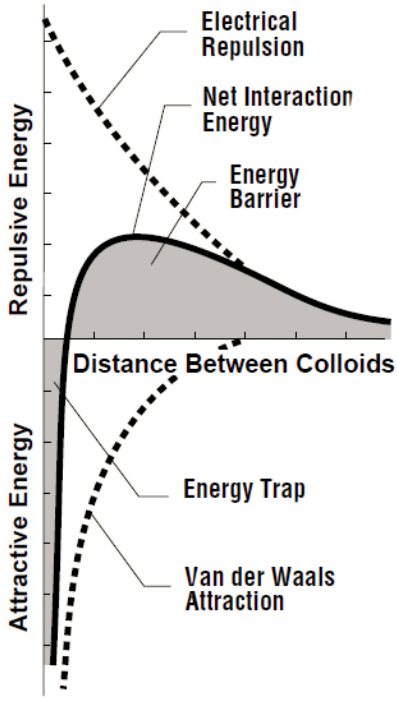

Figure 6.6. DLVO theory[76].

The distance between the particles determines the degree of the electrical repulsion or the Van der Waals attraction: The closer the particles, the greater the forces. The result of the combination of these two contrasting forces is DLVO, a theory that explains the tendency of a colloid to form or not to form aggregates as a function of the particle distance. The energy barrier is the result of the net interaction force, when the latter has a repulsive effect; the lower the energy barrier, the greater the coagulation. Depending on the substances, it will manifest first as "primary minimum", when the distance is very small and Van der Waals attraction is prevailing, then as "maximum" repulsion and, finally, as "secondary minimum".

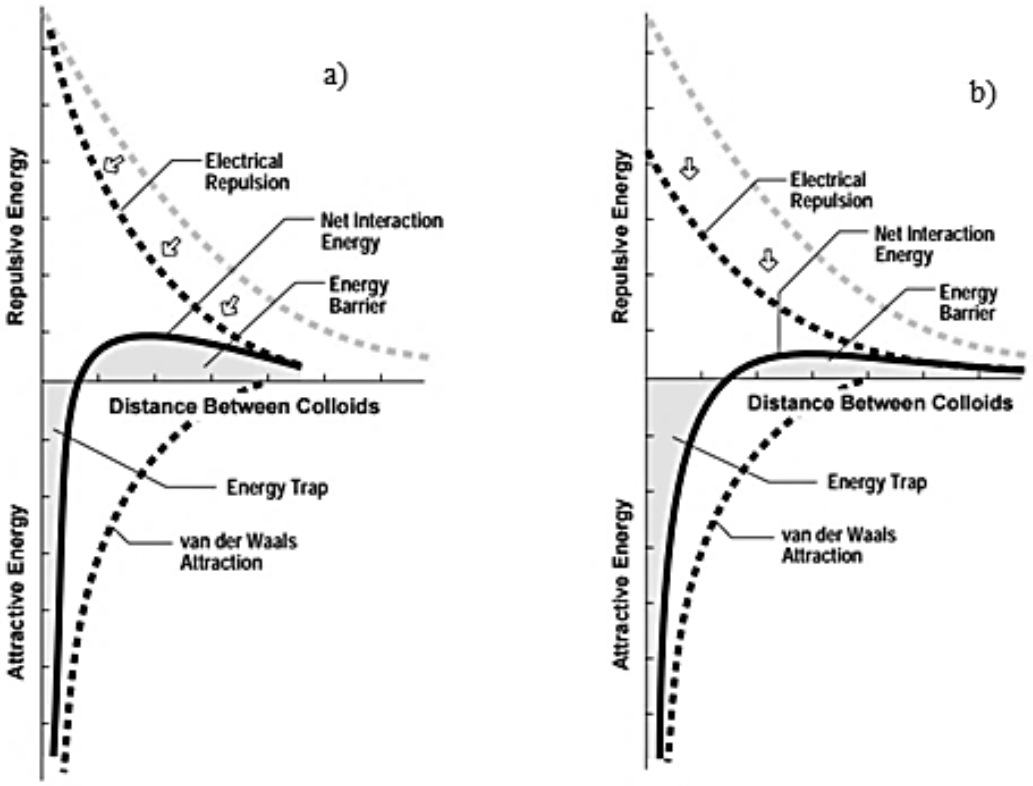

Figure 6.7. Double Layer compression (a) and lowering of the surface charge (b)[76].

The energy barrier is a function of the ionic concentration in the aquatic media (that is to say, ionic strength), of their valence, of the zeta potential, and of the particle size.

The energy barrier can be reduced:

- By increasing the ionic strength;

- By increasing the valence of the dispersed particles (Double Layer compression, Fig.6.7a); and

- By lowering the surface charge (Fig.6.7b) by means of reducing the zeta potential using coagulants.

In addition, the aggregation state of zinc oxide nanoparticles is influenced by the ionic strength (measured in mM) of the aqueous media. The ionic strength of an aqueous solution, as defined in the IUPAC's Gold Book[77], is the measure of the concentration of the ions in a solution. As mentioned in a study by Bian et al. (2011)[78], the aggregation of zinc oxide nanoparticles in an aqueous solution at neutral pH was found dependent on the ionic strength of the solution. Indeed, an incremental increase of the ionic strength corresponded to an incremental increase of the nanoparticle aggregation and sedimentation.

The isoelectric point (i.e., IEP) is the pH corresponding to zero charge in a molecule, i.e. zero zeta potential. The zeta potential is measured in millivolt (i.e., mV). At the isoelectric point, repulsive forces become weaker, and aggregation can take place. As reported by Marsalek in his study "Particle size and Zeta Potential of ZnO" (2014)[79], the isoelectric point of ZnO corresponds to a pH of 10, while zinc oxide nanoparticles with a zeta potential ranging from -30 mV to 30 mV can be classified as unstable, showing clear inclination toward particle aggregation.

Kanel et al. (2011)[80] investigated the isoelectric point of zinc oxide nanoparticles in their study "Influence of pH on the transport of nanoscale zinc oxide in saturated porous media". As can be seen in Figure 6.8, the isoelectric point (i.e., zeta potential equal to 0 mV) of nano-ZnO corresponded to a pH of 8.9.

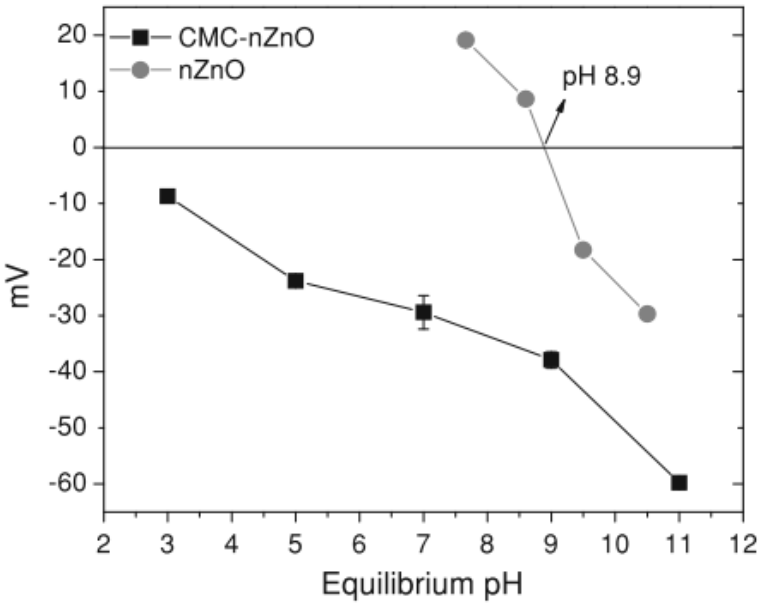

Figure 6.8. Isoelectric point of nano-ZnO.[80]

In the review conducted by Buzea et al. (2007)[65], it can be assessed that, when nanoparticles form aggregates, they tend to have lower toxic effects compared to the same nanoparticles not aggregated, even if present at higher concentration in the aqueous media. This could be justified by considering that the two nanoparticles will present different available surface area.

The study "Effect of ZnO nanoparticles aggregation on the toxicity in RAW 264.7 murine macrophage" by Tripathy et al. (2014)[81] indicates that, as a result of laboratory experiments, ZnO nanoparticles show a proportional relationship between concentration and aggregation. Indeed, an increment in the concentration induced a parallel increment in the effective diameter of the nanoparticles, as can be seen in Figure 6.9a, denoting the particles' tendency to aggregate. In addition, they tested the ionic dissolution deriving from both low-concentrated non-aggregated (LC-ZnO, 50 μg/mL) and high-concentrated aggregated HC-ZnO (300 μg/mL) ZnO nanoparticles. In Figure 6.9b it is possible to see the result of the experiment, showing that LC-ZnO generated a much higher concentration of Zn^{2+} throughout the experiments duration.

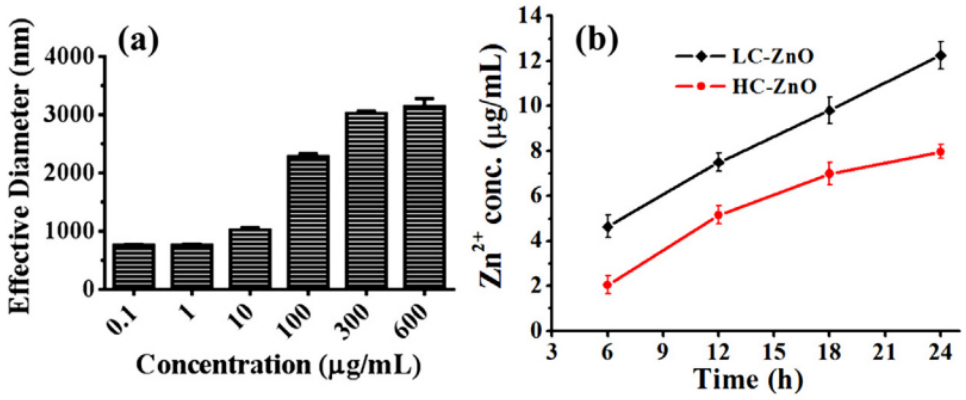

Figure 6.9. a) Effective diameter and ZnO concentration, b) Zn^{2+} concentration as a function of time for LC-ZnO and HC-ZnO.[81]

In light of those studies and the experimental outcomes reported in Chapter 3 and Chapter 4, it seems appropriate hypothesizing that aggregation took place when high concentrations of zinc oxide nanoparticles were added to the artificial seawater. As mentioned in Spisni and Seo et al. (2016, submitted)[58], *Thalassiosira pseudonana* exposed for 48 hours to 50 mg/L of industrial-derived zinc oxide nanoparticles showed a slight increase in particle size (from 1549 nm to 1574 nm), whereas when exposed to sunscreen-derived nano-ZnO the particle size increased from 1234 nm to 2217 nm. Besides, the zeta potential of *Thalassiosira pseudonana*, exposed to 50 mg/L of industrial-derived and sunscreen-derived nano-ZnO (0 and 48 hours after inoculation), can be seen in Table 6.2 (Spisni and Seo et al., 2016 submitted[58]): The decrease in zeta potential suggests a tendency toward particle aggregation.

	Zeta potential (mV)	
	0 hours	48 hours
Industrial nano-ZnO, 50 mg/L	-9.0	-8.5
Sunscreen nano-ZnO, 50 mg/L	-8.5	-4.0

Table 6.2. Zeta potential of polluted samples, 0 and 48 hours after inoculation[58].

In addition, the same study[58] shows Scanning Electron Microscopy (SEM) images of samples used in the growth inhibition experiments described the previous chapters.

The samples analyzed consisted in:

- Control sample (i.e. bare *Thalassiosira pseudonana* in artificial seawater);
- *Thalassiosira pseudonana* exposed to 50 mg/L of industrial-derived zinc oxide nanoparticles; and
- *Thalassiosira pseudonana* exposed to 50 mg/L of sunscreen-derived zinc oxide nanoparticles.

The analysis confirmed the presence of aggregated particles in the samples polluted with sunscreen-derived nanoparticles, and showed that both types of nanoparticles induced morphological changes in the diatom cells.

6.5 Surface area effect

As stated in IUPAC's Gold Book[77], the specific surface area of a particle is defined as "The surface area divided by the mass of the relevant phase," i.e., the surface area per unit of mass. The specific surface area of particles, and, specifically, nanoparticles, is what characterizes the rate of the reactions occurring at the phases interface, like the ionization of nano zinc oxide producing Zn^{2+} released in the aqueous media. Indeed, the reactions

$$ZnO\ (s) + H_2O\ (l) \leftrightarrow Zn(OH)_2\ (s)$$

$$Zn(OH)_2\ (s) \leftrightarrow Zn(OH)^+\ (aq) + OH^-\ (aq)$$

$$Zn(OH)^+\ (aq) \leftrightarrow Zn^{2+}\ (aq) + OH^-\ (aq)$$

are based on the exchange of electrons between zinc oxide and liquid water, making use of the contact between the two substances. As can be guessed, the availability of specific surface area is crucial to the reaction rate. According to Chang et al. (2012)[64], the larger the nanoparticle specific surface area , the greater:

- The nanoparticle accumulation;
- The reactivity; and

- The interaction between nanoparticles and other molecules.

The smaller the particle, the larger the (specific) surface area. Indeed, diminishing the size of the particle, i.e. its diameter, the available surface area will be subjected to an increment, as shown below in Figure 6.10.

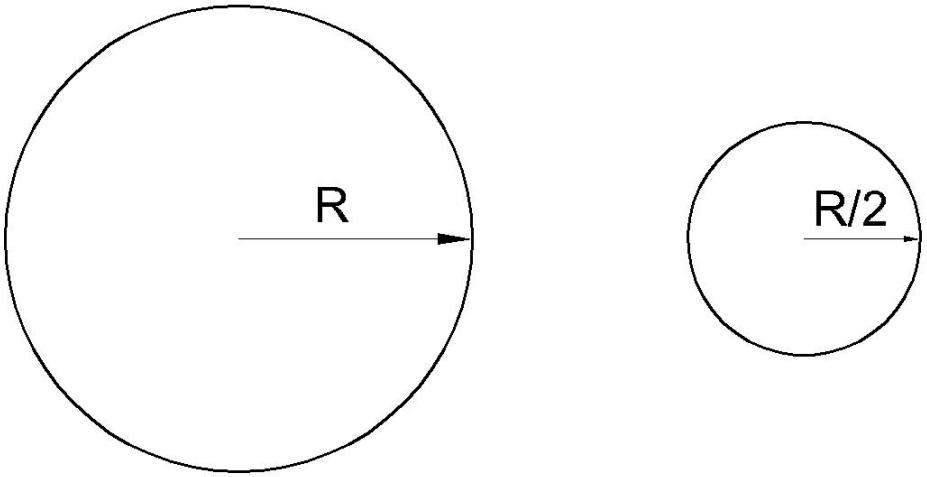

Figure 6.10. Surface area of two spheres.

Assuming that the two spheres in Figure 6.10 are made of the same material, the specific surface area is given by the surface area to volume ratio. The generic equation of the surface area and the volume of a sphere are, respectively,

$$\text{Surface Area } SA = 4\pi r^2$$

$$\text{Volume } V = \frac{4\pi r^3}{3}$$

The surface area to volume ratio is given by

$$\frac{SA}{V} = \frac{3}{r}$$

The surface area to volume of the first sphere, with r = R, is then equal to 3/R, while the surface area to volume of the second sphere, with r = R/2, is then equal to 6/R: By halving the radius of a particle, the specific surface area doubles. This is the reason why the small dimension of nanoparticles is a crucial factor and has to be taken into account when investigating the toxicity induced by them. Indeed, since

the macro, bulky version of the compound has a larger size, the ionization will be executed at different rates, given the lower reactivity derived from the lower specific surface area.

In the present case study, no bulk zinc oxide was tested. Although, industrial-derived and sunscreen-derived ZnO nanoparticles were sufficiently small and, in light of that, it appears reasonable supposing that their specific surface area was adequately large be involved into the toxic mechanisms; indeed, it is plausible that the large surface area fostered the nanoparticles' reactivity in artificial seawater, especially at low nano-ZnO concentrations, leading to the toxic effects observed throughout all the laboratory experiments.

6.6 Reactive Oxygen Species effect

As already mentioned in the first chapter, ROS are Reactive Oxygen Species. Those molecules contain oxygen and are highly reactive. Due to their nature, Reactive Oxygen Species can damage the cell my means of genetic modification and may also alter the ecosystem, by means of inhibition of phytoplankton's photosynthesis.

As mentioned by Fu et al. (2014)[69] in the study "Mechanisms of nanotoxicity: generation of reactive oxygen species", the ROS production depends on a multitude of physical and chemical properties of the specific metal oxide, including size and shape of the nanoparticle, surface are, oxidation status, presence of a coating, degree of aggregation and agglomeration, and other factors. In addition to the properties of the metal oxide compound, light exposure also plays a key role in ROS production: Sirelkhatim et al. (2015)[82] in their study "Review on Zinc Oxide Nanoparticles: Antibacterial Activity and Toxicity Mechanism" underline that nano-ZnO exposure to UV light will lead to the release of free radicals like superoxide anion (O_2^-), hydrogen peroxide (H_2O_2), and hydroxide (OH^-). The reactions that lead to the release of ROS are listed as follows:

$$ZnO + h\nu \rightarrow e^- + h^+$$

$$h^+ + H_2O \rightarrow {}^{\bullet}OH + H^+$$

$$e^- + O_2 \rightarrow {}^{\bullet}O_2^-$$

$${}^{\bullet}O_2 + H^+ \rightarrow HO_2^{\bullet}$$

$$HO_2^{\bullet} + H^+ + e^- \rightarrow H_2O_2$$

Where hν is the energy of a quantum of light, h^+ is an hole and the symbol $^{\bullet}$ represents the neutral form of the ion.

As highlighted by Devasagayam et al. (2004)[83] in their study "Free radicals and antioxidants in human health: current status and future prospects", Reactive Oxygen Species are naturally occurring in organisms and they play relevant roles at the cellular and molecular level. At this stage, ROS levels are maintained at adequate levels by antioxidants. The adverse effects brought by ROS become evident when their occurrence becomes greater than what is required by the organisms' vital functions, leading to an unbalanced oxidative stress.

The review by Fu et al. (2014)[69] also mentions the adverse effects induced by ROS generated by nanoparticles, as it is possible to see in Figure 6.11.

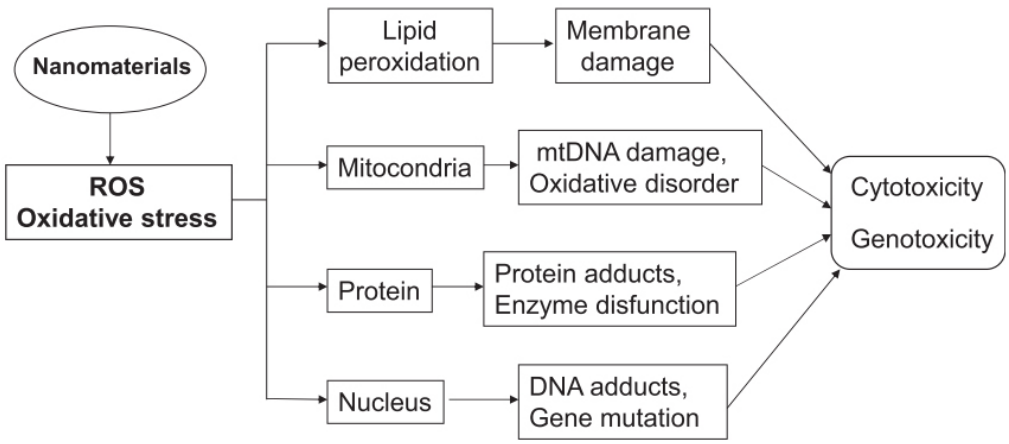

Figure 6.11. ROS toxic effects induced by nanomaterials[69].

As can be noticed, ROS species interact with the cellular health following multiple paths, involving many vital structures.

Regarding the Reactive Oxygen Species production induced by nano-ZnO, the study by Bhuvaneshwari et al. (2015)[66] indicates that the ROS generation is related

to both the concentration and the size of nanoparticles in the aqueous media. In particular, ROS production was assessed to be greater for increasing nano-ZnO concentrations. At the same time, ROS production was also estimated inversely proportional to the nanoparticles size: Experiments showed that the smaller the particle, the higher the Reactive Oxygen Species generation. Moreover, it can be noticed that nanoparticles exposed to UV-C light showed greater ROS production, compared to visible light and dark conditions. The overall effects on the ROS production influenced by nanoparticle concentration, nanoparticle size and light exposure, detected by Bhuvaneshwari et al. (2015)[66], are presented in Figure 6.12.

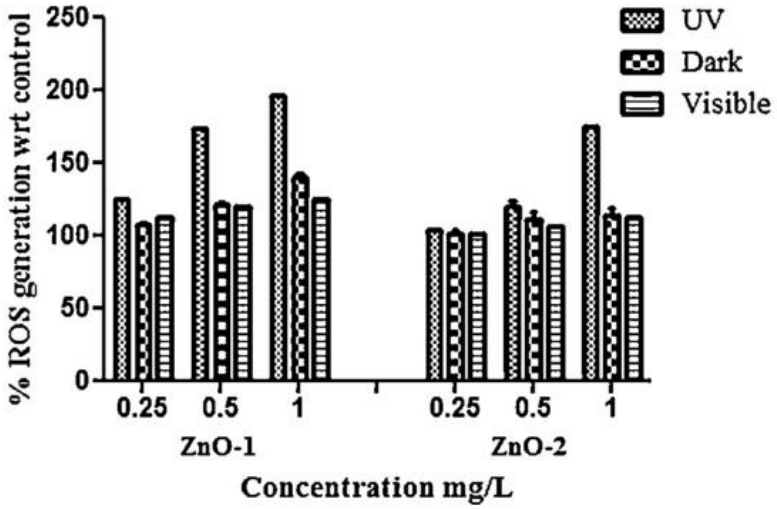

Figure 6.12. ROS production as a function of nano-ZnO size and concentration[66].

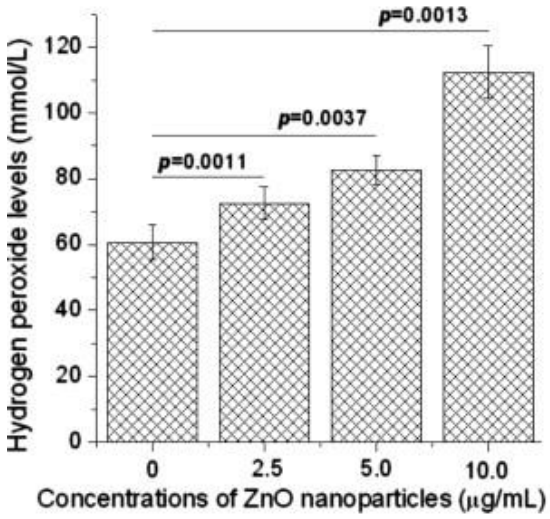

Figure 6.13. Hydrogen peroxide production vs. nano-ZnO concentration.[84]

Another study by Guo et al. (2013)[84] underlines the correlation between the increment of nano-ZnO concentration and the parallel enhanced hydrogen peroxide H_2O_2 production (Fig.6.13).

For what concerns the present case study, no ROS production assessment test was performed while investigating the toxicity induced by industrial-derived and sunscreen-derived zinc oxide nanoparticles toward the diatom *Thalassiosira pseudonana* in the Environmental Engineering Laboratory. However, the overall toxic effects can still be compared to the results available in literature. In particular it is possible to notice that:

- Higher concentration of both industrial-derived and sunscreen-derived zinc oxide nanoparticles in artificial seawater led to greater toxic effects, and this result is analogous to the ROS production literature; and
- Smaller, industrial-derived nanoparticles induced grater toxic effects (i.e. growth inhibition) at low concentrations toward the diatom, with respect to sunscreen-derived nanoparticles. Again, analogous results were found in ROS production literature.

As a conclusion, a multitude of factors (summarized in Table 6.3) might have influenced the toxicity of industrial-derived and sunscreen-derived nanoparticles toward *Thalassiosira pseudonana*, although the specific impact of every factor is not known, due to the complex physical, chemical and biological processes involved.

Factor	Present case study		Other studies	Bibliography
	Industrial-derived nano-ZnO	**Sunscreen-derived nano-ZnO**	**Industrial-derived nano-ZnO**	
Nanoparticle type	Greater growth inhibition w.r.t. sunscreen-derived nanoparticles, especially at low concentrations.	Lower growth inhibition w.r.t. industrial-derived nanoparticles, especially at low concentrations.	Induced growth inhibition, no comparison with sunscreen-derived available	Suman et al. (2015)[32] Manzo et al. (2013)[33]
Exposure time	Proportional; breakthrough time equal to 48 hours post inoculation.	Proportional; breakthrough time equal to 48 hours post inoculation.	Proportional; significant growth inhibition observed between 48 and 72 hours post inoculation.	Suman et al. (2015)[32] Luo (2007)[34]
Nanoparticle concentration	Slight effect considering exposure time, greater impact observed when fixing exposure time. Greater inhibition at higher concentration. May affect the degree of aggregation.	Slight effect considering exposure time, greater impact observed when fixing exposure time. Greater inhibition at higher concentration. May affect the degree of aggregation.	Greater inhibition at higher concentration.	Suman et al. (2015)[32] Manzo et al. (2013)[33] Luo (2007)[34] Adam et al. (2015)[35] Buzea et al. (2007)[65]
Particle Size and Shape	Relevant effects, leading mechanism at low nanoparticle concentration. Particle size equal to 24 nm. The smaller the particle, the greater the inhibition. Spherical particles.	Relevant effects, leading mechanism at low nanoparticle concentration. Particle size equal to 31 nm. The smaller the particle, the greater the inhibition. Spherical particles.	The smaller the particle, the greater the inhibition.	Bhuvaneshwari et al. (2015)[66] Kasemets et al. (2009)[67] Hund-Rinke et al. (2006)[68]

Ionic Dissolution	pH 8.5, dissolution is not considered a mechanism.	pH 8.5, dissolution is not considered a mechanism.	Zn^{2+} ions induce toxic effects and depend on the pH.	Chang et al. (2012)[64] Bhuvaneshwari et al. (2015)[66] Degen et al. (1999)[70] Miller et al. (2010)[71] Miao et al. (2010)[72]
Nanoparticle aggregation	Relevant aggregation at high nanoparticle concentration: The particle size becomes irrelevant. Aggregation at 50 mg/L (lower than sunscreen). Leading mechanism at high nanoparticle concentration.	Relevant aggregation at high nanoparticle concentration: The particle size becomes irrelevant. Aggregation at 50 mg/L (greater than industrial). Leading mechanism at high nanoparticle concentration.	Aggregated nanoparticles less toxic than non-aggregated nanoparticles. Aggregation proportional to nanoparticle concentration.	Buzea et al. (2007)[65] Marsalek (2014)[79] Kanel et al. (2011)[80] Tripathy et al. (2014)[81]
Nanoparticle surface area	Might affect the growth inhibition at low nanoparticle concentration, when particle size is the leading toxic mechanism.	Might affect the growth inhibition at low nanoparticle concentration, when particle size is the leading toxic mechanism.	Higher nanoparticle surface area corresponds to greater toxicity.	Chang et al. (2012)[64] Degen et al. (1999)[70]
ROS production	Not assessed, but results are compatible with bibliography.	Not assessed, but results are compatible with bibliography.	ROS production induced by photocatalysis, DNA damage.	Bhuvaneshwari et al. (2015)[66] Fu et al. (2014)[69] Sirelkhatim et al. (2015)[82] Devasagayam et al. (2004)[83] Guo et al. (2013)[84]

Table 6.3. Factors that might have influenced the growth inhibition.

Chapter 7 - Conclusions and future outlooks

The aim of this study was a preliminary estimation of the potential threat posed by different types of zinc oxide nanoparticles to the diatom *Thalassiosira pseudonana*, one of the simplest among many other aquatic organisms.

While industrial-derived zinc oxide nanoparticles were purchased from a vendor, sunscreen-derived nanoparticles were extracted in the laboratory (according to literature) from a commercially available sunscreen product. The results of the present case study, obtained performing the experiments in the Environmental Engineering Laboratory of the University of Miami, USA, are aligned with the available nanotoxicology bibliography up to date, although few studies regarding the growth inhibition induced by self-extracted nanosized metal oxides on aquatic species have been published nowadays.

The results of the experiments showed that smaller, industrial-derived nano-ZnO induces greater toxic effects toward the diatom with respect to sunscreen-derived nano-ZnO at each concentration and exposure time.

However, concentration is thought to play a significant role in the toxic mechanisms leading to growth inhibition: If nanoparticles are present in low concentration in the aquatic media, the toxicity is likely to be influenced by the nanoparticle size, whereas if the nanoparticles are present in higher concentrations, the toxicity is likely to be influenced by the aggregation state of the nanoparticles rather than by the size of the individual particles.

In addition, increasing the concentration of the nanoparticles in the aqueous media, the discrepancy between the growth inhibition induced by industrial- and sunscreen-derived nanoparticles becomes smaller.

Finally, the growth inhibition of the diatom was found to be dependent on the exposure time to the pollutant metal oxide nanoparticles: A longer exposure time corresponded to a greater growth inhibition induced by both types of zinc oxide nanoparticles, even though the toxic effects promoted by industrial-derived nano-ZnO were assessed to be greater with respect to those promoted by sunscreen-derived nano-ZnO.

The uniqueness of the present case study is represented by both the characterization and the comparison between the growth inhibition induced by industrial- and sunscreen-derived zinc oxide nanoparticles: The experiments showed that the two different types of nanoparticles have a similar behavior, even though sunscreen-derived nano-ZnO presented lower toxic effects to *Thalassiosira pseudonana*,

Although the available bibliography regarding the actual presence of zinc oxide nanoparticles in the environment suggests smaller concentration ranges, the present case study focuses on the theoretical issue posed by higher nano-ZnO concentrations, modeling both the accumulation of this metal oxide nanoparticle in the environment and the bioaccumulation induced by food chain mechanisms. Indeed, more complex aquatic organisms are fed on diatoms, and *Thalassiosira pseudonana* represents one of the most simple producer organisms of the aquatic food chain. Moreover, algae represent an invaluable source of oxygen for the entire ecosystem[40], hence it is extremely important to evaluate the potential threat posed by nanosized metal oxides contained in commercially available and widely used sun care products.

Further studies are undoubtedly needed, in order to have a more organic knowledge of the present topic. More in-depth research is required in order to unveil all the possible toxic mechanisms and the potential hazard posed by nanosized metal oxides toxicity toward food chain producers and, in general, toward the ecosystem.

The present case study focused on the toxicity induced by two different types of zinc oxide nanoparticles, as a function of their concentration in artificial seawater and their exposure time. Further nanotoxicological studies concerning the release of particles from commercially available products might be performed assessing:

- The hazard posed by different nanoparticles;
- The potential release of zinc oxide nanoparticles, as well as other nanosized metal oxide, from a different consumer product (e.g. paints, toothpastes, and other personal care products), by focusing on the mechanisms inducing the toxic effects;

- The extent of the toxic effects induced by nanoparticle size and shape, by means of X-ray Absorption Near Edge Structure (i.e., XANES) and Extended X-Ray Absorption Fine Structure (i.e., EXAFS)[85]; and

- The effect of stabilizers[80], like carboxymethyl cellulose (i.e., CMC), coating the nanoparticle's surface, on the growth inhibition of the diatom.

The carboxymethyl cellulose, coating the nanoparticle, acts as a stabilizer and promotes the dispersion of nanoparticles in the aqueous media. The effects induced by the presence of stabilizers, like CMC, coating the metal oxide nanoparticle released by commercially available products might be assessed by means of different instrumentation (e.g., Fourier transformed infrared (FTIR) spectroscopy[86]).

Works Cited

(1) Thomas, P. J. Nanoparticles. *Annu. Reports Sect. "A" (Inorganic Chem.* **2013**, *109*, 453.

(2) Discovery, S.; Future, T. H. E.; Medicine, O. F. Nanotechnology. **2015**, *313* (2), 2014–2015.

(3) Zielinski, A.; Sobieszczyk, S. Nanotechnologies in development of structural materials and biomaterials. *Adv. Mater. Sci.* **2011**, *11* (1).

(4) Roy, K.; Alam, M. N.; Mandal, S. K.; Debnath, S. C. Sol-gel derived nano zinc oxide for the reduction of zinc oxide level in natural rubber compounds. *J. Sol-Gel Sci. Technol.* **2014**, *70* (3), 378–384.

(5) Velmurugan, P.; Lee, S.-M.; Cho, M.; Park, J.-H.; Seo, S.-K.; Myung, H.; Bang, K.-S.; Oh, B.-T. Antibacterial activity of silver nanoparticle-coated fabric and leather against odor and skin infection causing bacteria. *Appl. Microbiol. Biotechnol.* **2014**, *98* (19), 8179–8189.

(6) Lee, J.-W.; Choi, J. O.; Jeong, J.-E.; Yang, S.; Ahn, S. H.; Kwon, K.-W.; Lee, C. S. Energy harvesting of flexible and translucent dye-sensitized solar cell fabricated by laser assisted nano particle deposition system. *Electrochim. Acta* **2013**, *103*, 252–258.

(7) Weerasinghe, H. C.; Sirimanne, P. M.; Franks, G. V.; Simon, G. P.; Cheng, Y. B. Low temperature chemically sintered nano-crystalline TiO2 electrodes for flexible dye-sensitized solar cells. *J. Photochem. Photobiol. A Chem.* **2010**, *213* (1), 30–36.

(8) Nasir, A.; Wang, S.; Friedman, A. The emerging role of nanotechnology in sunscreens: an update. *Expert Rev. Dermatol.* **2011**, *6*, 437+.

(9) Nohynek, G. J.; Lademann, J.; Ribaud, C.; Roberts, M. S. Grey goo on the skin? Nanotechnology, cosmetic and sunscreen safety. *Crit. Rev. Toxicol.* **2007**, *37* (3), 251–277.

(10) Kaida, T.; Kobayashi, K.; Adachi, M.; Suzuki, F. Optical characteristics of titanium oxide interference film and the film laminated with oxides and their applications for cosmetics. *J. Cosmet. Sci.* **2004**, *55* (2), 219–220.

(11) Moezzi, A.; McDonagh, A. M.; Cortie, M. B. Zinc oxide particles: Synthesis, properties and applications. *Chem. Eng. J.* **2012**, *185-186*, 1–22.

(12) Espitia, P. J. P.; Soares, N. de F. F.; Coimbra, J. S. dos R.; de Andrade, N. J.; Cruz, R. S.; Medeiros, E. A. A. Zinc oxide nanoparticles: synthesis, antimicrobial activity and food packaging applications. *Food Bioprocess Technol.* **2012**, *5* (5), 1447–1464.

(13) Zinc Oxide | Globe Multitrade http://www.globegroupbd.com/gmt/zinc-oxide (accessed May 12, 2016).

(14) Zincite - RARE08-20 - Sterling Mine - USA Mineral Specimen http://www.irocks.com/minerals/specimen/6218 (accessed May 12, 2016).

(15) Piccinno, F.; Gottschalk, F.; Seeger, S.; Nowack, B. Industrial production quantities and uses of ten engineered nanomaterials in Europe and the world. *J. Nanoparticle Res.* **2012**, *14* (9), 1–11.

(16) Bystrzejewska-Piotrowska, G.; Golimowski, J.; Urban, P. L. Nanoparticles: Their potential toxicity, waste and environmental management. *Waste Manag.* **2009**, *29* (9), 2587–2595.

(17) Gebel, T.; Foth, H.; Damm, G.; Freyberger, A.; Kramer, P.-J.; Lilienblum, W.; Röhl, C.; Schupp, T.; Weiss, C.; Wollin, K.-M.; et al. Manufactured nanomaterials: categorization and approaches to hazard assessment. *Arch. Toxicol.* **2014**, *88* (12), 2191–2211.

(18) Lewicka, Z. A.; Benedetto, A. F.; Benoit, D. N.; Yu, W. W.; Fortner, J. D.; Colvin, V. L. The structure, composition, and dimensions of TiO2 and ZnO nanomaterials in commercial sunscreens. *J. Nanoparticle Res.* **2011**, *13* (9), 3607–3617.

(19) Lewicka, Z. A.; Yu, W. W.; Oliva, B. L.; Contreras, E. Q.; Colvin, V. L. Photochemical behavior of nanoscale TiO2 and ZnO sunscreen ingredients. *J. Photochem. Photobiol. A Chem.* **2013**, *263*, 24–33.

(20) Serpone, N.; Dondi, D.; Albini, A. Inorganic and organic UV filters: Their role and efficacy in sunscreens and suncare products. *Inorganica Chim. Acta* **2007**, *360* (3), 794–802.

(21) Sánchez-Quiles, D.; Tovar-Sánchez, A. Are sunscreens a new environmental risk associated with coastal tourism? *Environment International*. Elsevier Ltd **2015**, pp 158–170.

(22) Diffey, B. I. Sunscreens and melanoma: the future looks bright. *Br. J. Dermatol.* **2005**, *153* (2), 378–381.

(23) Sánchez-Quiles, D.; Tovar-Sánchez, A. Sunscreens as a source of hydrogen peroxide production in coastal waters. *Environ. Sci. Technol.* **2014**, *48* (16), 9037–9042.

(24) Newman, M. D.; Stotland, M.; Ellis, J. I. The safety of nanosized particles in titanium dioxide- and zinc oxide-based sunscreens. *Journal of the American Academy of Dermatology*. Elsevier Inc **2009**, pp 685–692.

(25) Giokas, D. L.; Salvador, A.; Chisvert, A. UV filters: From sunscreens to human body and the environment. *TrAC - Trends Anal. Chem.* **2007**, *26* (5), 360–374.

(26) Yung, M. M. N.; Mouneyrac, C.; Leung, K. M. Y. Ecotoxicity of zinc oxide nanoparticles in the marine environment. *Encyclopedia of Nanotechnology*; **2015**; pp 1–8.

(27) Tovar-Sánchez, A.; Sánchez-Quiles, D.; Basterretxea, G.; Benede, J. L.; Chisvert, A.; Salvador, A.; Moreno-Garrido, I.; Blasco, J. Sunscreen products as emerging pollutants to coastal waters. *PLoS One* **2013**, *8* (6).

(28) Gottschalk, F.; Sun, T.; Nowack, B. Environmental concentrations of engineered nanomaterials: review of modeling and analytical studies. *Environ. Pollut.* **2013**, *181*, 287–300.

(29) Gottschalk, F.; Sonderer, T.; Scholz, R. W.; Nowack, B. Modeled environmental concentrations of engineered nanomaterials (TiO(2), ZnO, Ag, CNT, Fullerenes) for different regions. *Environ. Sci. Technol.* **2009**, *43* (24), 9216–9222.

(30) Gottschalk, F.; Sonderer, T.; Scholz, R. W.; Nowack, B. Possibilities and limitations of modeling environmental exposure to engineered nanomaterials by probabilistic material flow analysis. *Environ. Toxicol. Chem.* **2010**, *29* (5), 1036–1048.

(31) Boxall, A. B. A.; Tiede, K.; Chaudhry, Q.; Aitken, R.; Jones, A. D.; Jefferson, B.; Lewis, J. Current and future predicted exposure to engineered nanoparticles. **2007**.

(32) Suman, T. Y.; Radhika Rajasree, S. R.; Kirubagaran, R. Evaluation of zinc oxide nanoparticles toxicity on marine algae chlorella vulgaris through flow cytometric, cytotoxicity and oxidative stress analysis. *Ecotoxicol. Environ. Saf.* **2015**, *113*, 23–30.

(33) Manzo, S.; Miglietta, M. L.; Rametta, G.; Buono, S.; Di Francia, G. Toxic effects of ZnO nanoparticles towards marine algae Dunaliella tertiolecta. *Sci. Total Environ.* **2013**, *445-446*, 371–376.

(34) Luo, J. Toxicity and bioaccumulation of nanomaterial in aquatic species. *J US Stock. Jr. Water Prize. doi* **2007**, 1–16.

(35) Adam, N.; Schmitt, C.; De Bruyn, L.; Knapen, D.; Blust, R. Aquatic acute species sensitivity distributions of ZnO and CuO nanoparticles. *Sci. Total Environ.* **2015**, *526*, 233–242.

(36) Bai, W.; Zhang, Z.; Tian, W.; He, X.; Ma, Y.; Zhao, Y.; Chai, Z. Toxicity of zinc oxide nanoparticles to zebrafish embryo: a physicochemical study of toxicity mechanism. *J. Nanoparticle Res.* **2010**, *12* (5), 1645–1654.

(37) Hanna, S. K.; Miller, R. J.; Zhou, D.; Keller, A. A.; Lenihan, H. S. Accumulation and toxicity of metal oxide nanoparticles in a soft-sediment estuarine amphipod. *Aquat. Toxicol.* **2013**, *142-143*, 441–446.

(38) Brand, L. E. The salinity tolerance of forty-six marine phytoplankton isolates. *Estuar. Coast. Shelf Sci.* **1984**, *18* (5), 543–556.

(39) Hasle, G. R.; B.R., H. Some species of the centric diatom genus Thalassiosira studies in the light and electron microscopes. *Nov. Hedwigia Beihefte* **1970**, *31*, 559–597.

(40) Armbrust, E. V.; Berges, J. A.; Bowler, C.; Green, B. R.; Martinez, D.; Putnam, N. H.; Zhou, S.; Allen, A. E.; Apt, K. E.; Bechner, M.; et al. The genome of the diatom Thalassiosira pseudonana: ecology, evolution, and metabolism. *Science* **2004**, *306* (5693), 79–86.

(41) Yung, M. M. N.; Wong, S. W. Y.; Kwok, K. W. H.; Liu, F. Z.; Leung, Y. H.; Chan, W. T.; Li, X. Y.; Djurisic, A. B.; Leung, K. M. Y. Salinity-dependent toxicities of zinc oxide nanoparticles to the marine diatom Thalassiosira pseudonana. *Aquat. Toxicol.* **2015**, *165*, 31–40.

(42) Peng, X.; Palma, S.; Fisher, N. S.; Wong, S. S. Effect of morphology of ZnO nanostructures on their toxicity to marine algae. *Aquat. Toxicol.* **2011**, *102* (3-4), 186–196.

(43) Pérez-Cabero, M.; Puchol, V.; Beltrán, D.; Amorós, P. Thalassiosira pseudonana diatom as biotemplate to produce a macroporous ordered carbon-rich material. *Carbon N. Y.* **2008**, *46* (2), 297–304.

(44) Ellwood, M. J.; Hunter, K. A. The incorporation of zinc and iron into the frustule of the marine diatom Thalassiosira pseudonana. *Limnol. Oceanogr.* **2000**, *45* (7), 1517–1524.

(45) Yung, M. M. N.; Mouneyrac, C.; Leung, K. M. Y. Ecotoxicity of zinc oxide nanoparticles in the marine environment. *Encycl. Nanotechnol.* **2014**, 2075–2084.

(46) Fisher, N. S.; Jones, G. J.; Nelson, D. M. Effects of copper and zinc on growth, morphology, and metabolism of Asterionella japonica (Cleve) 1. *J. Exp. Mar. Bio. Ecol.* **1981**, *51* (1), 37–56.

(47) Research & Discovery | Clinical Diagnostics - Beckman Coulter, Inc. https://www.beckmancoulter.com/wsrportal/wsr/index.htm (accessed May 12, 2016).

(48) Zetasizer Nano ZS90 for particle size and zeta potential measurements http://www.malvern.com/en/products/product-range/zetasizer-range/zetasizer-nano-range/zetasizer-nano-zs90/default.aspx (accessed May 12, 2016).

(49) HappyLight Liberty 5K Natural Spectrum Energy Lamp http://www.verilux.com/light-therapy-lamps/happylight-liberty-5k-light-therapy/ (accessed May 12, 2016).

(50) Thermo Scientific Orion 720Aplus and 920Aplus pH/mV/ISE Benchtop Meters:Thermometers, https://www.fishersci.com/shop/products/thermo-scientific-orion-720aplus-920aplus-ph-mv-ise-benchtop-meters-2/p-194975 (accessed May 12, 2016).

(51) Guillard, R. R. L.; Ryther, J. H. Studies of marine planktonic ditoms: I. Cyclotella Nana Hustedt, and Deton Confervacea (Cleve) Gran. *Can. J. Microbiol.* **1962**, *8* (2), 229–239.

(52) Keller, M. D.; Seluin, R. C.; Claus, W.; Guillard, R. R. L.; Provasoli, L.; Pinter, I. J. Media for the culture of oceanic ultraphytoplankton. *Deep Sea Res. Part B. Oceanogr. Lit. Rev.* **1988**, *35* (6), 561.

(53) Zinc oxide nanopowder, <50 nm particle size (BET), >97% | Sigma-Aldrich http://www.sigmaaldrich.com/catalog/product/aldrich/677450?lang=en&region=US (accessed May 12, 2016).

(54) CCMP1335 | NCMA - Culturing Diversity https://ncma.bigelow.org/ccmp1335#.VzShffnhC00 (accessed May 12, 2016).

(55) Litchman, E.; Neale, P. J. UV effects on photosynthesis, growth and acclimation of an estuarine diatom and cryptomonad. *Mar. Ecol. Prog. Ser.* **2005**, *300* (Neale 2001), 53–62.

(56) Reynolds, R. A.; Stramski, D.; Kiefer, D. A. The effect of nitrogen limitation on the absorption and scattering properties of the marine diatom Thalassiosira pseudonana. *Limnol. Ocean.* **1997**, *42* (5), 881–892.

(57) Kiefer, D. A.; Olson, R. J.; Wilson, W. H. Reflectance spectroscopy of marine phytoplankton. Part 1. Optical properties as related to age and growth rate. *Limnol. Oceanogr.* **1979**, *24* (4), 664–672.

(58) Spisni, E.; Seo, S.; Joo, S. H.; Su, C. Release and toxicity comparison between industrial- and sunscreen-derived nano-ZnO particles. *Int. J. Environ. Sci. Technol.* (**2016**, submitted).

(59) Cao, P.; Cai, X.; Lu, W.; Zhou, F.; Huo, J. Growth inhibition and induction of apoptosis in SHG-44 glioma cells by chinese medicine formula “Pingliu Keli”. *Evid. Based. Complement. Alternat. Med.* **2011**, *2011*.

(60) Althouse, G. C.; Lu, K. G. Bacteriospermia in extended porcine semen. *Theriogenology* **2005**, *63* (2 SPEC. ISS.), 573–584.

(61) Walgreens Clear Zinc Sunscreen Broad Spectrum SPF 50 | Walgreens http://www.walgreens.com/store/c/walgreens-clear-zinc-sunscreen-broad-spectrum-spf-50/ID=prod6170803-product (accessed May 12, 2016).

(62) Barker, P. J.; Branch, A. The interaction of modern sunscreen formulations with surface coatings. *Prog. Org. Coatings* **2008**, *62* (3), 313–320.

(63) Bondarenko, O.; Juganson, K.; Ivask, A.; Kasemets, K.; Mortimer, M.; Kahru, A. Toxicity of Ag, CuO and ZnO nanoparticles to selected environmentally relevant test organisms and mammalian cells in vitro: A critical review. *Arch. Toxicol.* **2013**, *87* (7), 1181–1200.

(64) Chang, Y.-N.; Zhang, M.; Xia, L.; Zhang, J.; Xing, G. The toxic effects and mechanisms of CuO and ZnO nanoparticles. *Materials (Basel).* **2012**, *5* (12), 2850–2871.

(65) Buzea, C.; Pacheco, I. I.; Robbie, K. Nanomaterials and nanoparticles: sources and toxicity. *Biointerphases* **2007**, *2* (4), MR17–R71.

(66) Bhuvaneshwari, M.; Iswarya, V.; Archanaa, S.; Madhu, G. M.; Kumar, G. K. S.; Nagarajan, R.; Chandrasekaran, N.; Mukherjee, A. Cytotoxicity of ZnO NPs towards fresh water algae Scenedesmus obliquus at low exposure concentrations in UV-C, visible and dark conditions. *Aquat. Toxicol.* **2015**, *162* (December), 29–38.

(67) Kasemets, K.; Ivask, A.; Dubourguier, H.-C.; Kahru, A. Toxicity of nanoparticles of ZnO, CuO and TiO2 to yeast Saccharomyces cerevisiae. *Toxicol. In Vitro* **2009**, *23* (6), 1116–1122.

(68) Hund-Rinke, K.; Simon, M. Ecotoxic effect of photocatalytic active nanoparticles (TiO2) on algae and daphnids. *Environ. Sci. Pollut. Res. Int.* **2006**, *13* (4), 225–232.

(69) Fu, P. P.; Xia, Q.; Hwang, H.-M.; Ray, P. C.; Yu, H. Mechanisms of nanotoxicity: generation of reactive oxygen species. *J. food drug Anal.* **2014**, *22* (1), 64–75.

(70) Degen, A.; Kosec, M. Effect of pH and impurities on the surface charge of zinc oxide in aqueous solution. *J. Eur. Ceram. Soc.* **2000**, *20* (6), 667–673.

(71) Miller, R. J.; Lenihan, H. S.; Muller, E. B.; Tseng, N.; Hanna, S. K.; Keller, A. a. Impacts of metal oxide nanoparticles on marine phytoplankton. *Environ. Sci. Technol.* **2010**, *44* (19), 7329–7334.

(72) Miao, A. J.; Zhang, X. Y.; Luo, Z.; Chen, C. S.; Chin, W. C.; Santschi, P. H.; Quigg, A. Zinc oxide-engineered nanoparticles: Dissolution and toxicity to marine phytoplankton. *Environ. Toxicol. Chem.* **2010**, *29* (12), 2814–2822.

(73) *Compendium of Polymer Terminology and Nomenclature*; Jones, R. G., Wilks, E. S., Metanomski, W. V., Kahovec, J., Hess, M., Stepto, R., Kitayama, T., Eds.; The Royal Society of Chemistry, **2009**.

(74) Tindall Effect http://silver-lightning.com/tyndall/ (accessed May 12, 2016).

(75) Liese, A.; Hilterhaus, L. Evaluation of immobilized enzymes for industrial applications. *Chem. Soc. Rev.* **2013**, *42* (15), 6236–6249.

(76) Ravina, L.; Moramarco, N. Everything you want to know about Coagulation & Flocculation. *Zeta-Meter, Inc* **1993**, 1–37.

(77) IUPAC Gold Book online . *Chemistry International* . International Union of Pure and Applied Chemistry **2011**, p 20.

(78) Bian, S. W.; Mudunkotuwa, I. A.; Rupasinghe, T.; Grassian, V. H. Aggregation and dissolution of 4 nm ZnO nanoparticles in aqueous environments: Influence of pH, ionic strength, size, and adsorption of humic acid. *Langmuir* **2011**, *27* (10), 6059–6068.

(79) Marsalek, R. Particle Size and Zeta Potential of ZnO. *APCBEE Procedia* **2014**, *9*, 13–17.

(80) Kanel, S. R.; Al-Abed, S. R. Influence of pH on the transport of nanoscale zinc oxide in saturated porous media. *J. Nanoparticle Res.* **2011**, *13* (9), 4035–4047.

(81) Tripathy, N.; Hong, T.-K.; Ha, K.-T.; Jeong, H.-S.; Hahn, Y.-B. Effect of ZnO nanoparticles aggregation on the toxicity in RAW 264.7 murine macrophage. *J. Hazard. Mater.* **2014**, *270*, 110–117.

(82) Sirelkhatim, A.; Mahmud, S.; Seeni, A.; Kaus, N. H. M.; Ann, L. C.; Bakhori, S. K. M.; Hasan, H.; Mohamad, D. Review on zinc oxide nanoparticles: antibacterial activity and toxicity mechanism. *Nano-Micro Lett.* **2015**, *7* (3), 219–242.

(83) Devasagayam, T. P. a; Tilak, J. C.; Boloor, K. K.; Sane, K. S.; Ghaskadbi, S. S.; Lele, R. D. Free radicals and antioxidants in human health: current status and future prospects. *J. Assoc. Physicians India* **2004**, *52* (October), 794–804.

(84) Guo, D.; Bi, H.; Liu, B.; Wu, Q.; Wang, D.; Cui, Y. Reactive oxygen species-induced cytotoxic effects of zinc oxide nanoparticles in rat retinal ganglion cells. *Toxicol. Vitr.* **2013**, *27* (2), 731–738.

(85) Cheng, G.; Carter, J. D.; Guo, T. Investigation of Co nanoparticles with EXAFS and XANES. *Chem. Phys. Lett.* **2004**, *400* (1-3), 122–127.

(86) Joo, S. H.; Al-Abed, S. R.; Luxton, T. Influence of carboxymethyl cellulose for the transport of titanium dioxide nanoparticles in clean silica and mineral-coated sands. *Environ. Sci. Technol.* **2009**, *43* (13), 4954–4959.

ACKNOWLEDGMENT

I would like to express my deepest gratitude to my advisors, Professor Andrea Bolognesi from Università di Bologna and Professor Sung Hee Joo from University of Miami, for their guidance, support, valuable discussions and insightful comments.

I wish to thank Seokju Seo who helped me conducting experiments.

I wish to thank my parents for their love and full support, as well as Daniele Gasparri, Laura Khammash and my friends from the University of Bologna.

I also wish to express my appreciation to Andrea Galletti, Maria Arguelles, Kusumitha Perera, and all my classmates at the University of Miami for their support and friendship.